Available online at www.sciencedirect.com
SCIENCE DIRECT®
Journal of Magnetic Resonance 173 (2005) 236–253
JMR Journal of Magnetic Resonance
www.elsevier.com/locate/jmr

Algebraic description of spin 3/2 dynamics in NMR experiments

Costin Tanase[a,b,*], Fernando E. Boada[b,1]

[a] Department of Physics and Astronomy, University of Pittsburgh, 35905 O'Hara Street, Pittsburgh, PA 15213, USA
[b] MR Research Center, University of Pittsburgh Medical Center, 200 Lothrop Street, Pittsburgh, PA 15213, USA

Received 17 August 2004; revised 20 November 2004
Available online 23 January 2005

Abstract

The dynamics of spin 3/2 systems is analyzed using the density matrix theory of relaxation. By using the superoperator formalism, an algebraic formulation of the density matrix's evolution is obtained, in which the contributions from free relaxation and RF application are easily factored out. As an intermediate step, an exact form for the propagator of the density matrix for a spin 3/2 system, in the presence of static quadrupolar coupling, inhomogeneous static magnetic field, and relaxation is demonstrated. Using this algebraic formulation, exact expressions for the behavior of the density matrix in the classical one-, two-, and three-pulse experiments are derived. These theoretical formulas are then used to illustrate the bias introduced on the measured relaxation parameters by the presence of large spatial variations in the B_0 and B_1 fields. The theoretical predictions are easily evaluated through simple matrix algebra and the results agree very well with the experimental observations. This approach could prove useful for the characterization of the spatial variations of the signal intensity in multiple quantum-filtered sodium MRI experiments.

Keywords: Sodium; Multiple quantum filter; Relaxation; Quadrupolar nuclei; Coherence

1. Introduction

The NMR behavior of spin 3/2 systems is particularly interesting in the context of biological systems because of the dependence of their NMR signal on the electrical and structural properties of the biological microenvironment. This dependence has been exploited in the context of multiple quantum-filtered (MQF) sodium NMR experiments for the study of ion fluxes during ischemia experiments and for the identification of neoplastic changes in human tissue [1,2]. Imaging extensions of these NMR techniques, although highly desirable, are not as common in the literature because of the low concentration of sodium in human tissue and the inherent challenges involved in the fast spatial encoding of the sodium NMR signal [3].

Fortunately, the development of efficient spatial encoding techniques in MRI [4] has allowed the generation of sodium images in times that are adequate for practical use in humans (data acquisition time less than 10 min). Extensions of these techniques have also been used to provide the first demonstration of in vivo MQF sodium MRI techniques in humans [5,6]. The routine application of MQF techniques for the non-invasive diagnosis and monitoring of pathology in humans, however, requires a more thorough understanding of the dependence of this novel image contrast on hard-to-control spatial variations in experimental parameters such as the B_1 field and the B_0 field. Such understanding can only be attained through a proper description of the behavior of the spin system for arbitrary values of the aforementioned experimental parameters.

The standard theoretical approach for describing the spin dynamics in the presence of non-negligible

* Corresponding author. Fax: +1 4126479800.
E-mail addresses: tanc@phyast.pitt.edu, huiduhu@yahoo.com (C. Tanase).
[1] Supported in part by PHS Grants, 1R2187805, 1R01HL64205, and 1R01000291.

1090-7807/$ - see front matter © 2005 Elsevier Inc. All rights reserved.
doi:10.1016/j.jmr.2004.12.009

relaxation behavior is based on the Redfield equations [7]. Analytic solutions for the Redfield equations can be obtained by reducing the Redfield equations to a system of linear differential equations in a suitably chosen basis of quantum mechanical operators. These approaches, however, do not reveal inherent factorizations of the solution. Such factorizations are attractive for practical use because of the natural separation they provide for the effects of the experimental parameters on the signal.

In this work, we demonstrate that by using the superoperator formalism [8], the solution to the Redfield equations can be reduced to a purely algebraic calculation in which the coherence pathways leading to the measured signal can be easily identified. This approach offers two additional advantages. First, each pathway contribution can be expressed as a product of simple terms representing the succession of RF pulses and RF-free evolutions that is typical of pulsed MQF experiments. Second, the associated expressions are constructed in a basis-free form.

The paper starts by reviewing many of the relevant properties of a spin 3/2 system in the superspace representation. The superspace formulation of the Redfield equations is then presented and used to construct the propagator for the spin system's evolution in the absence of the RF field. This is followed by a description of the RF excitation in the superoperator space. The superspace formalism is then used to derive the expressions for the time dependence of the NMR signal for the classical one-, two-, and three-pulse NMR experiments. These expressions are then used to model the experimentally acquired signals from agar gels phantoms, because such gels offer the isotropic, slow fluctuating environment necessary for bi-exponential relaxation behavior of sodium. The anisotropic case, while contained in the theoretical description, it is not experimentally investigated in this work. The paper concludes with a discussion of the advantages and potential limitations of the proposed techniques.

2. Theory

2.1. The spin 3/2 superspace

The quantum mechanical description of isolated 3/2 spins is constructed in the Hilbert space H associated with the $j = 3/2$ irreducible representation of the rotation group. In this space of dimension $N = 4$, the natural basis is the angular momentum basis $\{|jm\rangle\}$ with $j = 3/2$, $m = -3/2, \ldots, 3/2$. In the Hilbert space description, the pure states are described as four dimensional vectors, while the mixed states are described by matrices.

The Liouville representation of quantum mechanics is introduced to treat both types of states in a common fashion. In this representation, the states (pure or mixed) are described as self-adjoint, positive-defined operators with unit trace [8]. Due to the finite dimensionality of H, both the state space and the observable space (the space of bounded operators acting on H) can be embedded in the linear space of $N \times N$ matrices. Following [9], this N^2 dimensional space is called superspace (or Liouville space) and is denoted S. The elements of S are sometimes referred to as supervectors.

In superspace, the double "ket" $|O\rangle\rangle$ and double "bra" $\langle\langle O|$ denote the N^2 dimensional vectors describing the operator 'O' and its hermitic conjugate '$O^\dagger$', respectively. The Liouville space becomes an unitary space when it is equipped with the natural inner product [9]

$$\langle\langle A|B\rangle\rangle \equiv \mathrm{Tr}\{A^\dagger B\}. \tag{1}$$

The linear operators acting on S are called superoperators. A special class of superoperators is defined by the operation of taking the commutator. The derivation with respect to O [9], is denoted using the corresponding bold face $\mathbf{O} : \mathsf{S} \to \mathsf{S}$, and is acting on arbitrary operators B as the commutator

$$\mathbf{O}|B\rangle\rangle = |C\rangle\rangle \quad \text{with } C = [O, B]. \tag{2}$$

For the particular case of the Hamiltonian, the associated commutator superoperator is the Liouvillian, which is denoted by $\mathbf{L}$.

From an algebraic point of view, the superspace is associated with the direct product of two $j = 3/2$ representations of the rotation group. The product reduces to a direct sum of representations labeled with principal quantum numbers $l = 0, 1, 2, 3$. Therefore, the quantum mechanical operators can be expanded in terms of the normalized spherical irreducible tensor (SIT) operators $T_{lm}, l = 0, 1, 2, 3, m = -l, \ldots l$, [8,10]. For the sake of simplicity, the notations $|lm\rangle\rangle \equiv |T_{lm}\rangle\rangle, \langle\langle lm| \equiv \langle\langle T^\dagger_{lm}|$ are used. The SIT's satisfy

$$\begin{aligned} &\mathbf{J}_Z|lm\rangle\rangle = m|lm\rangle\rangle, \\ &\langle\langle lm|\lambda\mu\rangle\rangle = \delta_{l\lambda}\delta_{m\mu}, \quad \sum_{l=0}^{3}\sum_{m=-l}^{l}|lm\rangle\rangle\langle\langle lm| = \mathbf{1}_{16}. \end{aligned} \tag{3}$$

The decomposition of general operators and superoperators in terms of SIT's can be written:

$$\begin{aligned} &|B(t)\rangle\rangle = \sum_{l,m}|lm\rangle\rangle\langle\langle lm|B(t)\rangle\rangle, \\ &\mathbf{B} = \sum_{\lambda,\mu}\sum_{l,m}|lm\rangle\rangle\langle\langle lm|\mathbf{B}|\lambda\mu\rangle\rangle\langle\langle\lambda\mu| \end{aligned} \tag{4}$$

with the coefficients being given by the traces:

$$\begin{aligned} &\langle\langle lm|B\rangle\rangle = \mathrm{Tr}\{T^\dagger_{lm}B\}, \\ &\langle\langle lm|\mathbf{B}|\lambda\mu\rangle\rangle = \mathrm{Tr}\{T^\dagger_{lm}[B, T_{\lambda\mu}]\}. \end{aligned} \tag{5}$$

The axial symmetry, translated in the commutation of a given superoperator with the superoperator $\mathbf{J}_Z$, has important implications for the matrix elements of the superoperator, and it is used extensively in this paper

$$\langle\langle lm|[\mathbf{B},\mathbf{J}_Z]|\lambda\mu\rangle\rangle = 0 \Rightarrow \langle\langle lm|\mathbf{B}|\lambda\mu\rangle\rangle = \delta_{m\mu}\langle\langle lm|\mathbf{B}|\lambda m\rangle\rangle. \tag{6}$$

From here, the general representation of a superoperator, Eq. (4), is simplified; in terms of its reduced matrix elements $B^m_{l\lambda} \equiv \langle\langle lm|\mathbf{B}|\lambda m\rangle\rangle$ it reads

$$\mathbf{B} = \sum_{m=-3}^{3}\sum_{l=|m|}^{3}\sum_{\lambda=|m|}^{3} |lm\rangle\rangle B^m_{l\lambda}\langle\langle\lambda m|. \tag{7}$$

Grouping the terms with the same magnetic quantum number

$$\mathbf{B} = |00\rangle\rangle B^0_{00}\langle\langle 00| + \sum_{l=1}^{3}\sum_{\lambda=1}^{3}|l0\rangle\rangle B^0_{l\lambda}\langle\langle\lambda 0| + \sum_{m=1}^{3}\sum_{l=m}^{3} \times \sum_{\lambda=m}^{3}\left(|lm\rangle\rangle B^m_{l\lambda}\langle\langle\lambda m| + |l,-m\rangle\rangle B^{-m}_{l\lambda}\langle\langle\lambda,-m|\right), \tag{8}$$

one notes that any superoperator, commuting with the Z component of the angular momentum superoperator, has a block diagonal structure in the SIT basis.

$$\mathbf{B} = \text{blockdiag} \times (B^0_{00} \quad \mathbf{B}^{(0)} \quad \mathbf{B}^{(1)} \quad \mathbf{B}^{(2)} \quad \mathbf{B}^{(3)} \quad \mathbf{B}^{(-1)} \quad \mathbf{B}^{(-2)} \quad \mathbf{B}^{(-3)})$$

$$\mathbf{B}^{(k)} = \begin{pmatrix} B^k_{11} & B^k_{12} & B^k_{13} \\ B^k_{21} & B^k_{22} & B^k_{23} \\ B^k_{31} & B^k_{32} & B^k_{33} \end{pmatrix}, \quad k = 0, \pm 1,$$

$$\mathbf{B}^{(\pm 2)} = \begin{pmatrix} B^{\pm 2}_{22} & B^{\pm 2}_{23} \\ B^{\pm 2}_{32} & B^{\pm 2}_{33} \end{pmatrix}, \quad \mathbf{B}^{(\pm 3)} = \left(B^{\pm 3}_{33}\right). \tag{9}$$

The component $l = m = 0$ is purposely separated from the larger $m = 0$ subspace because the non-trivial dynamics take place in the 15 dimensional space spanned by operators with non-vanishing principal quantum number, $l \neq 0$. Therefore, from now on, all references to the $j = 3/2$ superspace are restricted to this fifteen dimensional space. The blocks corresponding to a given magnetic number m have dimensions $d(m) = 4 - |m|$ for non-zero m and $d(m) = 3$, for $m = 0$.

The block decomposition is explicitly revealed if one defines the matrices $\mathbf{e}_m$ which have as columns the SIT supervectors with the given m, in ascending order of principal index l

$$\mathbf{e}_m = \{||m|,m\rangle\rangle, ||m|+1,m\rangle\rangle \cdots, |3,m\rangle\rangle\} \text{ if } m \neq 0,$$
$$\mathbf{e}_0 = \{|10\rangle\rangle, |20\rangle\rangle, |30\rangle\rangle\}. \tag{10}$$

In terms of the individual blocks, the decomposition expressed by Eq. (9) is rewritten

$$\mathbf{B} = \sum_{m=-3}^{3} \mathbf{e}_m \mathbf{B}^{(m)} \mathbf{e}_m^{\mathrm{T}}. \tag{11}$$

Based on the multiplication properties of the introduced $\mathbf{e}_m$ matrices

$$\mathbf{e}_m^{\mathrm{T}}\mathbf{e}_m = \mathbf{1}_{d(m)\times d(m)}, \quad \mathbf{e}_m^{\mathrm{T}}\mathbf{e}_n = \mathbf{0}_{d(m)\times d(n)}, \tag{12}$$

the computation of a function of a superoperator $\mathbf{B}$ is reduced to a direct sum of functions of lower dimensional matrices

$$f(\mathbf{B}) = \sum_{m=-3}^{3} \mathbf{e}_m f(\mathbf{B}^{(m)}) \mathbf{e}_m^{\mathrm{T}}. \tag{13}$$

Further simplifications can be obtained if one considers the properties of the parity superoperator. Using the properties of the SIT's under inversion, the matrix elements of the parity superoperator, denoted $\mathbf{\Pi}$, are simply given by [11]

$$\langle\langle l,-m|\mathbf{\Pi}|lm\rangle\rangle = (-)^l. \tag{14}$$

If an operator $\mathbf{B}$ commutes with the pair $\mathbf{\Pi}$, $\mathbf{J}_Z$ further simplifications in the matrix element's structure in Eq. (6) occur

$$[\mathbf{\Pi},\mathbf{B}] = 0 \Rightarrow \mathbf{\Pi}\mathbf{B}\mathbf{\Pi} = \mathbf{B} \Rightarrow \langle\langle l,-m|\mathbf{B}|\lambda,-m\rangle\rangle = (-)^{l+\lambda}\langle\langle lm|\mathbf{B}|\lambda m\rangle\rangle. \tag{15}$$

While the reduction to lower dimensions is rigorously expressed by Eqs. (11) and (13), the notations are inconvenient for algebraic manipulation. Therefore, a simpler notation namely

$$\mathrm{e}_m \mathbf{B}^{(m)} \equiv \mathbf{e}_m \mathbf{B}^{(m)} \mathbf{e}_m^{\mathrm{T}} \tag{16}$$

is used in this paper.

2.2. The physical system

For most models used in biological applications, the Liouvillian describing the spin 3/2 system is given as a sum of four terms representing: interaction with static magnetic field B_0, static quadrupolar interaction, interaction with the rotating RF field B_1 and a term describing quadrupolar fluctuations [12]

$$\mathbf{L}^L(t) = -\omega_0\mathbf{J}_z + \omega_Q\mathbf{T}_{20} + \omega_1(t)\mathbf{J}_{\omega t+\varphi} + \sum_{q=-2}^{2}(-)^q\mathbf{T}_{2q}\mathbf{V}_{2,-q}. \tag{17}$$

Here, the frequencies $\omega_0 = |\gamma B_0|$, $\omega_1 = |\gamma B_1|$ are defined by the static and RF magnetic field magnitudes, ω_1 is the frequency of the applied RF field while ω_Q describes the strength of residual quadrupolar interaction [13]. We also use the convenient notation [14]

$$\mathbf{J}_\varphi = \mathbf{J}_x\cos\varphi + \mathbf{J}_y\sin\varphi. \tag{18}$$

Finally, the expressions for the quadrupolar and fluctuating terms are constructed using the standard approach described in [12,13,15]. The spin 3/2 system is interacting with an external, large system, assumed in

thermal equilibrium at a temperature T. In the case of a semiclassical description of relaxation, the fluctuations $V_{2,q}$ are considered stochastic complex functions of time with zero average and known correlation properties.

To distinguish between the laboratory and rotating frame, the density matrices in the laboratory and rotating frames are denoted with the letters σ and ρ, respectively. In the laboratory frame, the Liouville–von Neumann equation is easily cast into an explicit linear system of equations using the superspace formulation, that is

$$\frac{\mathrm{d}}{\mathrm{d}t}|\sigma(t)\rangle\rangle = -\mathrm{i}\mathbf{L}^L(t)|\sigma(t)\rangle\rangle. \tag{19}$$

The laboratory frame Liouvillian, Eq. (17), consists of a sum of three deterministic terms, $\mathbf{L}_0^L = -\omega_0\mathbf{J}_Z$, $\mathbf{L}_Q^L = \omega_Q\mathbf{T}_{20}$, $\mathbf{L}_{\mathrm{RF}}^L(t) = \omega_1(t)\mathbf{J}_{\omega t+\varphi}$ and the fluctuating part $\mathbf{F}^L(t) = \sum(-)^q\mathbf{T}_{2q}V_{2,-q}(t)$. The first two contributions are used to redefine the static interaction $\mathbf{L}_{\mathrm{S}}^L = -\omega_0\mathbf{J}_Z^L + \omega_Q\mathbf{L}_Q^L$.

The transition to the rotating frame is given, according to Eq. (A.15) from Appendix A.1, by the unitary transformation

$$|\sigma(t)\rangle\rangle = \exp(-\mathrm{i}\omega t\mathbf{J}_z)|\rho(t)\rangle\rangle \tag{20}$$

which together with the definition of the B_0 inhomogeneity parameter, $\delta \equiv \omega_0 - \omega$, reduces Eq. (19) to the form

$$\frac{\mathrm{d}}{\mathrm{d}t}|\rho(t)\rangle\rangle = -\mathrm{i}\left(-\delta\mathbf{J}_z + \omega_Q\mathbf{T}_{20} + \omega_1(t)\mathbf{J}_\varphi + \sum_{q=-2}^{2}(-)^q\mathrm{e}^{-\mathrm{i}q\omega t}V_{2,-q}(t)\mathbf{T}_{2q}\right)|\rho(t)\rangle\rangle. \tag{21}$$

Thus, to describe the dynamics of a spin 3/2 system in a typical pulsed NMR experiment, one needs to solve this stochastic equation in two different regimes, the free relaxation case (when the RF field is absent) and the hard pulse regime (in which a very strong RF field is applied). In the free relaxation case, the starting point is the equation in the laboratory frame, where the correlation functions of the fluctuations are easily computed

$$\frac{\mathrm{d}}{\mathrm{d}t}|\sigma(t)\rangle\rangle = -\mathrm{i}\left(-\omega_0\mathbf{J}_z + \omega_Q\mathbf{T}_{20} + \sum_{q=-2}^{2}(-)^q\mathbf{T}_{2q}V_{2,-q}(t)\right)|\sigma(t)\rangle\rangle, \tag{22}$$

while for the hard pulse regime when all but the RF contributions are neglected, the starting equation takes its simplest form in the rotating frame

$$\frac{\mathrm{d}}{\mathrm{d}t}|\rho(t)\rangle\rangle = -\mathrm{i}\omega_1(t)\mathbf{J}_\varphi|\rho(t)\rangle\rangle. \tag{23}$$

This last approximation of Eq. (21) assumes that the magnitude of the applied B_1 field is much larger than the magnitudes of the off-resonance, quadrupolar and fluctuation terms, and that the RF pulse length is much shorter than the characteristic relaxation times of the system.

2.3. Free relaxation

The approach to thermal equilibrium can only be obtained in a full quantum mechanical description of both the 3/2 spin system and the thermal bath. This is accomplished by considering the fluctuation's amplitudes as quantum mechanical operators acting on the Hilbert space associated with the thermal bath.

The semiclassical theory, obtained by considering the fluctuations as classical stochastic variables, requires the ad hoc introduction of thermal equilibrium [16]. In the high temperature case and in the presence of a strong static magnetic field, the equilibrium density matrix takes the form of the Maxwell–Boltzmann distribution

$$\sigma_{\mathrm{Eq}} = \frac{1}{Z}\exp\left(-\frac{\hbar\omega_0 J_Z}{k_{\mathrm{B}}T}\right) \quad \text{with} \quad Z = \mathrm{Tr}\left\{\exp\left(-\frac{\hbar\omega_0 J_Z}{k_{\mathrm{B}}T}\right)\right\}. \tag{24}$$

Separating the solution of the Liouville equation, Eq. (22), into its deterministic (σ_{D}) and fluctuating (σ_{F}) components

$$|\sigma(t)\rangle\rangle = |\sigma_{\mathrm{D}}(t)\rangle\rangle + |\sigma_{\mathrm{F}}(t)\rangle\rangle, \tag{25}$$

the evolution towards thermal equilibrium imposes the limit condition

$$\lim_{t\to\infty}\sigma_{\mathrm{D}}(t) = \sigma_{\mathrm{Eq}}. \tag{26}$$

Due to the strong static magnetic field assumption, the dynamical shift contributions are negligible, and the deterministic component of the density matrix satisfies the differential equation (16)

$$\frac{\mathrm{d}}{\mathrm{d}t}|\sigma_{\mathrm{D}}(t)\rangle\rangle = -\mathrm{i}\mathbf{L}_{\mathrm{S}}^L|\sigma_{\mathrm{D}}(t)\rangle\rangle - R(|\sigma_{\mathrm{D}}(t)\rangle\rangle). \tag{27}$$

The relaxation function, a linear function in the density matrix, is proved to satisfy the relation $\mathrm{R}(\sigma_{\mathrm{Eq}}) = 0$, in accordance with the Boltzmann form of thermal equilibrium. In the case of high temperatures, in pulse NMR experiments, the difference $\sigma_{\mathrm{D}}(t) - \sigma_{\mathrm{Eq}}$ can be assumed to be of first order in $\hbar\omega_0/k_{\mathrm{B}}T$. By neglecting terms of second order in $\hbar\omega_0/k_{\mathrm{B}}T$ (violating, in this order, the detailed balance relations) Eq. (27) is written [16]

$$\frac{\mathrm{d}}{\mathrm{d}t}(|\sigma_{\mathrm{D}}(t)\rangle\rangle - |\sigma_{\mathrm{Eq}}\rangle\rangle) = -\mathrm{i}\mathbf{L}_{\mathrm{S}}^L(|\sigma_{\mathrm{D}}(t)\rangle\rangle - |\sigma_{\mathrm{Eq}}\rangle\rangle) - \mathbf{R}(|\sigma_{\mathrm{D}}(t)\rangle\rangle - |\sigma_{\mathrm{Eq}}\rangle\rangle). \tag{28}$$

The relaxation superoperator, $\mathbf{R}$, is constructed in terms of the static Liouvillian as the average over fluctuations. The steps involved in this derivation are well known, [17] here the derivation is briefly exposed in superspace language. First, the differential equation

involving the full density matrix (deterministic and fluctuating part) [22] is rewritten in interaction picture in respect with the static Liouvillian

$$\frac{\mathrm{d}}{\mathrm{d}t}|\sigma'(t)\rangle\rangle = -\mathrm{i}\mathbf{F}'(t)|\sigma'(t)\rangle\rangle$$
$$\mathbf{F}'(t) = \exp(-\mathrm{i}\mathbf{L}_{\mathrm{S}}^{L}t)\mathbf{F}^{L}(t)\exp(\mathrm{i}\mathbf{L}_{\mathrm{S}}^{L}t)\ |\sigma'(t)\rangle\rangle = \exp(-\mathrm{i}\mathbf{L}_{\mathrm{S}}^{L}t)|\sigma(t)\rangle\rangle. \tag{29}$$

Second, the differential equation is converted to the integral representation

$$|\sigma'(t)\rangle\rangle = |\sigma'(0)\rangle\rangle - \mathrm{i}\int_0^t \mathrm{d}t_1\mathbf{F}'(t_1)|\sigma'(0)\rangle\rangle - \int_0^t \mathrm{d}t_1 \times \int_0^{t_1} \mathrm{d}t_2\mathbf{F}'(t_1)\mathbf{F}'(t_2)|\sigma'(t_2)\rangle\rangle. \tag{30}$$

The averaging over fluctuations, denoted by $\langle\rangle$, followed by the time derivative reduces the former expression to a mixed integral-differential equation (the fluctuations have zero mean, therefore the term linear in fluctuations disappear)

$$\frac{\mathrm{d}}{\mathrm{d}t}|\sigma'_{\mathrm{D}}(t)\rangle\rangle = |\sigma'_{\mathrm{D}}(0)\rangle\rangle - \int_0^t \mathrm{d}t_2\langle\mathbf{F}'(t)\mathbf{F}'(t_2)\rangle|\sigma'_{\mathrm{D}}(t_2)\rangle\rangle - \int_0^t \mathrm{d}t_2\langle\mathbf{F}'(t)\mathbf{F}'(t_2)|\sigma'_{\mathrm{F}}(t_2)\rangle\rangle\rangle. \tag{31}$$

The last term is neglected; in the second term, the assumption of short correlation time of fluctuations allows the replacement of the density matrix at integration point t_2 with the value at the moment t

$$\frac{\mathrm{d}}{\mathrm{d}t}|\sigma'_{\mathrm{D}}(t)\rangle\rangle = -\int_0^t \mathrm{d}\tau\langle\mathbf{F}'(t)\mathbf{F}'(\tau)\rangle|\sigma'_{\mathrm{D}}(t)\rangle\rangle. \tag{32}$$

Returning to the laboratory frame

$$\frac{\mathrm{d}}{\mathrm{d}t}|\sigma_{\mathrm{D}}(t)\rangle\rangle = -\mathrm{i}\mathbf{L}_{\mathrm{S}}^{L}|\sigma_{\mathrm{D}}(t)\rangle\rangle - \mathbf{R}(t)|\sigma_{\mathrm{D}}(t)\rangle\rangle \tag{33}$$

with the time dependent operator

$$\mathbf{R}(t) = \int_0^t \mathrm{d}\tau\langle\mathbf{F}^{L}(t)\exp(\mathrm{i}\mathbf{L}_{\mathrm{S}}^{L}(t-\tau))\mathbf{F}^{L}(\tau) \times \exp(-\mathrm{i}\mathbf{L}_{\mathrm{S}}^{L}(t-\tau))\rangle\rangle. \tag{34}$$

For weak quadrupolar interactions the static Liouvillian is dominated by the B_0 contribution in the exponentials and we thus obtain

$$\mathbf{R}(t) = \int_0^t \mathrm{d}\tau\langle\mathbf{F}^{L}(t)\exp(-\mathrm{i}\omega_0\mathbf{J}_Z(t-\tau))\mathbf{F}^{L}(\tau) \times \exp(\mathrm{i}\omega_0\mathbf{J}_Z(t-\tau))\rangle\rangle. \tag{35}$$

By using the form of the fluctuations, $\mathbf{F}^{L}(t) = \sum(-)^q \mathbf{T}_{2q}V_{2,-q}(t)$, the form imposed by the axial symmetry for the correlation functions

$$\langle V_{2,k}(t_1)V_{2,q}(t_2)\rangle = (-1)^q\delta_{k,-q}J_k(t_1-t_2), \tag{36}$$

and the transformation of the SIT superoperators under rotations (A.11)

$$\exp(-\mathrm{i}\omega_0\mathbf{J}_Z(t-\tau))\mathbf{T}_{2q}\exp(\mathrm{i}\omega_0\mathbf{J}_Z(t-\tau)) = e^{\mathrm{i}\omega_0 q(t-\tau)}\mathbf{T}_{2q}, \tag{37}$$

the relaxation operator is reduced to the form

$$\mathbf{R}(t) = \sum_{q=-2}^{2}(-1)^q\mathbf{T}_{2,q}\mathbf{T}_{2,-q}\int_0^t \mathrm{d}\tau J_q(t-\tau) \times \exp(-\mathrm{i}q\omega_0(t-\tau)). \tag{38}$$

When the time dependence of the previous expression is analyzed, it shows a very fast variation around $t = 0$, attaining its limit value $\mathbf{R}(\infty)$ on a time scale of order of the correlation time of fluctuations (much shorter than the time scale characterizing the relaxation) As a consequence, the upper limit in the integral can be replaced with the infinity giving rise to the symmetrized spectral functions (the anti-symmetric combinations are one order higher in $h\omega_0/k_{\mathrm{B}}T$) [13]

$$\mathbf{R} = \sum_{q=-2}^{2}(-1)^q(\mathbf{T}_{2,q}\mathbf{T}_{2,-q} + \mathbf{T}_{2,-q}\mathbf{T}_{2,q})j_q(q\omega_0). \tag{39}$$

Finally, by performing the replacement of the density matrix with the correct form (that a quantum mechanical treatment of the bath would predict) $\sigma_{\mathrm{D}} - \sigma_{\mathrm{Eq}}$, and by taking in consideration that the equilibrium density matrix belongs to the null space of the static Liouvillian

$$\mathbf{L}_{\mathrm{S}}^{L}|\sigma_{\mathrm{Eq}}\rangle\rangle = 0, \tag{40}$$

the evolution in the absence of the RF field, is described by a linear equation with time independent coefficients

$$\frac{\mathrm{d}}{\mathrm{d}t}(|\sigma_{\mathrm{D}}(t)\rangle\rangle - |\sigma_{\mathrm{Eq}}\rangle\rangle) = -(\mathrm{i}\omega_0\mathbf{J}_z + \mathrm{i}\omega_Q\mathbf{T}_{20} + j_0\mathbf{R}_0 + j_1\mathbf{R}_1 + j_2\mathbf{R}_2)(|\sigma_{\mathrm{D}}(t)\rangle\rangle - |\sigma_{\mathrm{Eq}}\rangle\rangle), \tag{41}$$

where the individual relaxation matrices are defined by products of superoperators associated with SITs

$$\mathbf{R}_0 = \mathbf{T}_{2,0}\mathbf{T}_{2,0},$$
$$\mathbf{R}_1 = -(\mathbf{T}_{2,1}\mathbf{T}_{2,-1} + \mathbf{T}_{2,-1}\mathbf{T}_{2,1}), \tag{42}$$
$$\mathbf{R}_2 = \mathbf{T}_{2,2}\mathbf{T}_{2,-2} + \mathbf{T}_{2,-2}\mathbf{T}_{2,2}.$$

Each individual term in the relaxation superoperator commutes with the superoperator for the Z-component of the angular momentum

$$[\mathbf{J}_Z, \mathbf{T}_{2m}\mathbf{T}_{2,-m}] = [\mathbf{J}_Z, \mathbf{T}_{2m}]\mathbf{T}_{2,-m} + \mathbf{T}_{2m}[\mathbf{J}_Z, \mathbf{T}_{2,-m}] = (m-m)\mathbf{T}_{2m}\mathbf{T}_{2,-m} = 0, \tag{43}$$

reducing the rotating frame analog of Eq. (41) to the form

$$\frac{\mathrm{d}}{\mathrm{d}t}(|\rho(t)\rangle\rangle - |\rho_{\mathrm{Eq}}\rangle\rangle) = -(\mathrm{i}\delta\mathbf{J}_z + \mathrm{i}\omega_Q\mathbf{T}_{20} + j_0\mathbf{R}_0 + j_1\mathbf{R}_1 + j_2\mathbf{R}_2)(|\rho(t)\rangle\rangle - |\rho_{\mathrm{Eq}}\rangle\rangle). \tag{44}$$

All terms in the Liouvillian and relaxation superoperator commute with $\mathbf{\Pi}$, therefore, the direct sum representation can be written (using the convenient notation introduced by Eq. (16))

$$\begin{aligned}
\mathbf{R}_0 &= (\mathrm{e}_1+\mathrm{e}_{-1})\mathbf{R}_0^{(1)} + (\mathrm{e}_2+\mathrm{e}_{-2})\mathbf{1}_2,\\
\mathbf{R}_1 &= \mathrm{e}_0\mathbf{R}_1^{(0)} + (\mathrm{e}_1+\mathrm{e}_{-1})\mathbf{1}_3 + (\mathrm{e}_2+\mathrm{e}_{-2})(\mathbf{1}_2+\mathbf{J}_Z) + (\mathrm{e}_3+\mathrm{e}_{-3}),\\
\mathbf{R}_2 &= \mathrm{e}_0\mathbf{R}_2^{(0)} + (\mathrm{e}_1+\mathrm{e}_{-1})\mathbf{R}_2^{(1)} + (\mathrm{e}_2+\mathrm{e}_{-2})\mathbf{1}_2 + (\mathrm{e}_3+\mathrm{e}_{-3}),\\
\mathbf{L}_Q &= (-\mathrm{e}_1+\mathrm{e}_{-1})\mathbf{L}_Q^{(1)} + (-\mathrm{e}_2+\mathrm{e}_{-2})\mathbf{J}_X,
\end{aligned} \tag{45}$$

$$\begin{aligned}
\mathbf{R}_1^{(0)} &= \frac{2}{5}\begin{pmatrix} 1 & 0 & 2\\ 0 & 1 & 0\\ 2 & 0 & 4\end{pmatrix}, \quad \mathbf{R}_2^{(0)} = \frac{2}{5}\begin{pmatrix} 4 & 0 & -2\\ 0 & 1 & 0\\ -2 & 0 & 1\end{pmatrix},\\
\mathbf{R}_0^{(1)} &= \frac{1}{5}\begin{pmatrix} 3 & 0 & \sqrt{6}\\ 0 & 1 & 0\\ \sqrt{6} & 0 & 2\end{pmatrix}, \quad \mathbf{R}_2^{(1)} = \frac{1}{5}\begin{pmatrix} 2 & 0 & -\sqrt{6}\\ 0 & 2 & 0\\ -\sqrt{6} & 0 & 3\end{pmatrix},\\
\mathbf{L}_Q^{(1)} &= \frac{-1}{\sqrt{5}}\begin{pmatrix} 0 & \sqrt{3} & 0\\ \sqrt{3} & 0 & \sqrt{2}\\ 0 & \sqrt{2} & 0\end{pmatrix}.
\end{aligned} \tag{46}$$

The solution of Eq. (44) is constructed for any initial condition, by using the forward propagator, defined by the matrix equation

$$\begin{cases} \frac{\mathrm{d}}{\mathrm{d}t}\mathbf{U}_\delta(\omega_Q, j_0, j_1, j_2, t) = -(\mathrm{i}\delta\mathbf{J}_z + \mathrm{i}\omega_Q\mathbf{T}_{20} + j_0\mathbf{R}_0 + j_1\mathbf{R}_1 \\ \qquad\qquad + j_2\mathbf{R}_2)\mathbf{U}_\delta(\omega_Q, j_0, j_1, j_2, t),\\ \mathbf{U}_\delta(\omega_Q, j_0, j_1, j_2, 0) = \mathbf{1}_{15}. \end{cases} \tag{47}$$

The solution of this equation is obtained through the matrix exponential

$$\begin{aligned}\mathbf{U}_\delta(\omega_Q, j_0, j_1, j_2, t) = \exp(-(\mathrm{i}\delta\mathbf{J}_z + i\omega_Q\mathbf{T}_{20} + j_0\mathbf{R}_0 \\ + j_1\mathbf{R}_1 + j_2\mathbf{R}_2)t).\end{aligned} \tag{48}$$

Once this quantity is computed, the evolution of the full density matrix takes an *inhomogeneous* linear form, symbolized here by the operation $\widetilde{\mathbf{U}}(t)\bullet$ and defined by the following equation:

$$\begin{aligned}|\rho(t_2)\rangle\rangle &= \widetilde{\mathbf{U}}_\delta(t_2-t_1)\bullet|\rho(t_1)\rangle\rangle\\ &= \mathbf{U}_\delta(t_2-t_1)(|\rho(t_1)\rangle\rangle - |\rho_{\mathrm{Eq}}\rangle\rangle) + |\rho_{\mathrm{Eq}}\rangle\rangle.\end{aligned} \tag{49}$$

The inhomogeneous term emerges only in the longitudinal component of the density matrix in the form of a time dependent function denoted $\rho_{\mathrm{rec}}(\mathrm{t})$, $|\rho_{\mathrm{rec}}(t)\rangle\rangle = (\mathbf{1} - \mathbf{U}_\delta(t))|\rho_{\mathrm{Eq}}\rangle\rangle$

$$|\rho(t_2)\rangle\rangle = \mathbf{U}_\delta(t_2-t_1)|\rho(t_1)\rangle\rangle + |\rho_{\mathrm{rec}}(t_2-t_1)\rangle\rangle. \tag{50}$$

2.4. Free propagator

The closed form of the propagator is the subject of this section. Its construction uses the axial symmetry (already explored in Section 2.1) and straightforward properties of projectors.

If $\mathbf{A}$ commutes with a projector $\mathbf{P}$ (an operator satisfying $\mathbf{P}^2 = \mathbf{P}$), then, for any analytic function f, in terms of the projector and its complement $\mathbf{Q} = \mathbf{1} - \mathbf{P}$ we can write

$$f(\mathbf{A}) = \mathbf{P}f(\mathbf{PA}) + \mathbf{Q}f(\mathbf{QA}). \tag{51}$$

Specific cases are the decomposition $\mathbf{A} = \mathbf{PA} + \mathbf{QA}$, the exponentiation of such operators

$$\exp(\alpha\mathbf{A}) = \mathbf{P}\exp(\alpha\mathbf{PA}) + \mathbf{Q}\exp(\alpha\mathbf{QA}) \tag{52}$$

and the exponentiation of a projector itself

$$\exp(\alpha\mathbf{P}) = \mathbf{P}\mathrm{e}^\alpha + \mathbf{Q} = \mathbf{1} + \mathbf{P}(\mathrm{e}^\alpha - 1). \tag{53}$$

The first factorization, relating the general propagator $\mathbf{U}_\delta$ with the on-resonance ($\delta = 0$) propagator, denoted simply $\mathbf{U}$, is obtained using the commutation of the Liouvillian with $\mathbf{J}_Z$

$$\mathbf{U}_\delta(\omega_Q, j_0, j_1, j_2, t) = \exp(-\mathrm{i}\delta t\mathbf{J}_Z)\mathbf{U}(\omega_Q, j_0, j_1, j_2, t). \tag{54}$$

The $\mathbf{R}_0$ matrix is a projector, this fact can be verified either from the general commutation relations, Eq. (A.12), or from its explicit form, Eq. (45). In terms of the orthogonal complement $\mathbf{P}_0 = \mathbf{1} - \mathbf{R}_0$, according to Eq. (52), the commutation of the Liouvillian with $\mathbf{R}_0$ implies

$$\exp(-t\mathbf{L}) = \mathbf{R}_0\exp(-t\mathbf{R}_0\mathbf{L}) + \mathbf{P}_0\exp(-t\mathbf{P}_0\mathbf{L}). \tag{55}$$

The $\mathbf{P}_0$ component of the propagator is computed using mutual orthogonal projectors $\mathbf{P}_{0i}$, $\mathbf{P}_{0i}\mathbf{P}_{0j} = \delta_{ij}\mathbf{P}_{0i}$

$$\begin{aligned}
\mathbf{P}_{01} &= \mathbf{P}_0(\mathbf{R}_1 - \mathbf{R}_2)(\mathbf{R}_1 - \mathbf{R}_2 + \mathbf{2})/8,\\
\mathbf{P}_{02} &= \mathbf{P}_0(\mathbf{R}_1 - \mathbf{R}_2)(\mathbf{R}_1 - \mathbf{R}_2 - \mathbf{2})/8,\\
\mathbf{P}_{03} &= \mathbf{P}_0(\mathbf{R}_1 + \mathbf{R}_2 - \mathbf{2})/8,\\
\mathbf{P}_{04} &= \mathbf{P}_0 - (\mathbf{P}_{01} + \mathbf{P}_{02} + \mathbf{P}_{03}),
\end{aligned} \tag{56}$$

in terms of which the $\mathbf{P}_0$ component of the Liouvillian can be written

$$\mathbf{P}_0\mathbf{L} = 2j_1\mathbf{P}_{01} + 2j_2\mathbf{P}_{02} + 2(j_1+j_2)\mathbf{P}_{03} + (j_1+j_2)\mathbf{P}_{04}. \tag{57}$$

The exponentiation is obtained from (52).

$$\mathbf{P}_0\mathrm{e}^{-t\mathbf{P}_0\mathbf{L}} = \mathbf{P}_{01}\mathrm{e}^{-2j_1t} + \mathbf{P}_{02}\mathrm{e}^{-2j_2t} + \mathbf{P}_{03}\mathrm{e}^{-2(j_1+j_2)t} + \mathbf{P}_{04}\mathrm{e}^{-(j_1+j_2)t}. \tag{58}$$

For the $\mathbf{R}_0$ component, the following operators commuting with $\mathbf{R}_0$ are defined, with $\alpha = 1, 2$

$$\begin{aligned}
&\mathbf{K}_{\alpha3} = \mathbf{R}_0(\mathbf{R}_\alpha - \mathbf{1})/2, \quad \mathbf{K}_{\alpha1} = 2\mathbf{K}_{\alpha3}\mathbf{T}_{20}\mathbf{K}_{\alpha3},\\
&\mathbf{K}_{\alpha2} = -2\mathrm{i}\mathbf{K}_{\alpha3}\mathbf{K}_{\alpha1}.
\end{aligned} \tag{59}$$

They satisfy the commutation relations of two independent $s = 1/2$ spins

$$[\mathbf{K}_{1i}, \mathbf{K}_{2j}] = 0, (i, j = 1, 2, 3),$$
$$[\mathbf{K}_{\beta 1}, \mathbf{K}_{\beta 2}] = \mathrm{i}\mathbf{K}_{\beta 3}, \quad \text{and circular permutations.} \tag{60}$$

Using those spin-like operators, the $\mathbf{R}_0$ component of the Liouvillian can be written

$$\mathbf{R}_0\mathbf{L} = (j_0 + j_1 + j_2)\mathbf{R}_0 + 2\sum_{\alpha=1,2}(j_\alpha \mathbf{K}_{\alpha 3} - \omega_Q \mathbf{K}_{\alpha 1}) \tag{61}$$

and its exponentiation reads

$$\mathbf{R}_0 \mathrm{e}^{-t\mathbf{R}_0\mathbf{L}} = \mathrm{e}^{-(j_0+j_1+j_2)t}\mathbf{R}_0 \sum_{\alpha=1,2}\mathbf{M}_\alpha \quad \text{with}$$
$$\mathbf{M}_\alpha = \exp[-2t(j_\alpha \mathbf{K}_{\alpha 3} - \omega_Q \mathbf{K}_{\alpha 1})]. \tag{62}$$

The final exponentials are well known from Pauli matrix algebra, with $\Delta_\alpha = \sqrt{j_\alpha^2 - \omega_Q^2}$

$$\mathbf{M}_\alpha = \mathbf{M}_\alpha(\omega_Q, j_\alpha, t) = \frac{\mathrm{sh}(t\Delta_\alpha)}{\Delta_\alpha}(j_\alpha(1 - \mathbf{R}_\alpha) - \mathrm{i}\omega_Q \mathbf{T}_{20}(1 - \mathbf{R}_\alpha)^2) + \mathrm{ch}(t\Delta_\alpha)(1 - \mathbf{R}_\alpha)^2. \tag{63}$$

The final formula for longitudinal and transversal components, in a basis-free formulation, reads

$$\mathbf{U}^L(j_1, j_2, t) = \mathbf{P}_{01}\mathrm{e}^{-2j_1 t} + \mathbf{P}_{02}\mathrm{e}^{-2j_2 t} + \mathbf{P}_{03}\mathrm{e}^{-2(j_1+j_2)t},$$
$$\mathbf{U}^{\mathrm{T}}(j_0, j_1, j_2, \omega_Q, t) = \mathrm{e}^{-(j_1+j_2)t}\mathbf{P}_{04} + \mathrm{e}^{-(j_0+j_1+j_2)t}\mathbf{R}_0 \sum_{\alpha=1,2}\mathbf{M}_\alpha(\omega_Q, j_\alpha, t). \tag{64}$$

The 'basis-free' syntagma used here has the meaning that, regardless of the basis choice in the Liouville space, once the set of SIT superoperators T_{lm} is constructed, the free propagator can be obtained by mechanically following the succession of transformations described by Eqs. (42), (56), (59), and (64).

One of the frequently encountered cases is the relaxation in isotropic environments, where $\omega_Q \to 0$ simultaneously with $j_1 \to j_2$. In this situation, $\Delta_\alpha \to j_\alpha$ and, with the auxiliary notations $f(t) = \mathrm{e}^{-t(j_0+j_2)}$, $s(t) = \mathrm{e}^{-2tj_2}$, the propagator takes the form

$$\mathbf{U}(j_0, j_2, j_2, 0, t) = s\mathbf{P}_0 - s(1 - s)\mathbf{P}_{03} + 2f\left((1 + s)(\mathbf{K}_{13}^2 + \mathbf{K}_{23}^2) - \frac{1}{2}(1 - s)(\mathbf{K}_{13} + \mathbf{K}_{23})\right). \tag{65}$$

Using the axial symmetry and parity considerations the structure of the propagator is expressed in terms of fourteen functions $u_{l\lambda}^m, 0 \leqslant m \leqslant \lambda \leqslant l \leqslant 3$

$$\mathbf{U} = \begin{pmatrix} u_{11}^0 & 0 & u_{31}^0 \\ 0 & u_{22}^0 & 0 \\ u_{31}^0 & 0 & u_{33}^0 \end{pmatrix}\mathbf{e}_0 + \begin{pmatrix} u_{11}^1 & u_{21}^1 & u_{31}^1 \\ u_{21}^1 & u_{22}^1 & u_{32}^1 \\ u_{31}^1 & u_{32}^1 & u_{33}^1 \end{pmatrix}\mathbf{e}_1 + \begin{pmatrix} u_{11}^1 & -u_{21}^1 & u_{31}^1 \\ -u_{21}^1 & u_{22}^1 & -u_{32}^1 \\ u_{31}^1 & -u_{32}^1 & u_{33}^1 \end{pmatrix}\mathbf{e}_{-1} + \begin{pmatrix} u_{22}^2 & u_{32}^2 \\ u_{32}^2 & u_{33}^2 \end{pmatrix}\mathbf{e}_2 + \begin{pmatrix} u_{22}^2 & -u_{32}^2 \\ -u_{32}^2 & u_{33}^2 \end{pmatrix}\mathbf{e}_{-2} + u_{33}^3(\mathbf{e}_3 + \mathbf{e}_{-3}). \tag{66}$$

In the case of zero quadrupolar splitting, the structure simplifies, requiring only ten functions

$$\mathbf{U} = \begin{pmatrix} u_{11}^0 & 0 & u_{31}^0 \\ 0 & u_{22}^0 & 0 \\ u_{31}^0 & 0 & u_{33}^0 \end{pmatrix}\mathbf{e}_0 + \begin{pmatrix} u_{11}^1 & 0 & u_{31}^1 \\ 0 & u_{22}^1 & 0 \\ u_{31}^1 & 0 & u_{33}^1 \end{pmatrix}\mathbf{e}_1 + \begin{pmatrix} u_{11}^1 & 0 & u_{31}^1 \\ 0 & u_{22}^1 & 0 \\ u_{31}^1 & 0 & u_{33}^1 \end{pmatrix}\mathbf{e}_{-1} + \begin{pmatrix} u_{22}^2 & 0 \\ 0 & u_{33}^2 \end{pmatrix}\mathbf{e}_2 + \begin{pmatrix} u_{22}^2 & 0 \\ 0 & u_{33}^2 \end{pmatrix}\mathbf{e}_{-2} + u_{33}^3(\mathbf{e}_3 + \mathbf{e}_{-3}). \tag{67}$$

Comparing this expression with Eq. (64) and the explicit expression of the auxiliary projectors Eqs. ((A.16)–(A.20)) the individual matrix elements are easily found, and they are presented in Appendix A.2.

2.5. Hard pulse

After a hard RF pulse, with flip angle θ and phase φ applied at a time t, the density matrix $\rho(t_+)$ is given in terms of the density matrix before the pulse, $\rho(t_-)$, by the formula

$$|\rho(t_+)\rangle\rangle = \mathbf{P}(\theta, \varphi)|\rho(t_-)\rangle\rangle = \exp(\mathrm{i}\theta\mathbf{J}_\varphi)|\rho(t_-)\rangle\rangle. \tag{68}$$

Equivalent expressions are useful in symbolic calculations

$$\mathbf{P}(\theta, \varphi) = \exp(-\mathrm{i}\varphi\mathbf{J}_Z)\exp(\mathrm{i}\theta\mathbf{J}_X)\exp(\mathrm{i}\varphi\mathbf{J}_Z) = \exp\left(-\mathrm{i}\left(\varphi - \frac{\pi}{2}\right)\mathbf{J}_Z\right)\exp(\mathrm{i}\theta\mathbf{J}_Y) \times \exp\left(\mathrm{i}\left(\varphi - \frac{\pi}{2}\right)\mathbf{J}_Z\right). \tag{69}$$

In the SIT basis, the matrix elements define the reduced p functions by

$$\langle\langle lm|\mathbf{P}(\theta, \phi)|\lambda\mu\rangle\rangle = \mathrm{e}^{\mathrm{i}(\mu-m)\phi}\langle\langle lm|\mathrm{e}^{-\mathrm{i}\theta\mathbf{J}_X}|\lambda\mu\rangle\rangle = \delta_{l\lambda}\mathrm{e}^{\mathrm{i}(\mu-m)\phi}p_\lambda^{m\mu}(\theta). \tag{70}$$

The standard notations in quantum mechanics are given using the exponentiation of the Y component of the angular momentum, by using the second part of Eq. (69) the same matrix element can be expressed

$$\langle\langle lm|\mathbf{P}(\theta, \phi)|\lambda\mu\rangle\rangle = \exp\left(\mathrm{i}(\mu - m)\left(\phi - \frac{\pi}{2}\right)\right)\langle\langle lm|\mathrm{e}^{-\mathrm{i}\theta\mathbf{J}_Y}|\lambda\mu\rangle\rangle = \delta_{l\lambda}\mathrm{e}^{\mathrm{i}(\mu-m)\phi}(i)^{m-\mu}d_\lambda^{m\mu}(\theta), \tag{71}$$

where $d_{m\mu}^l(\theta)$ are the well-known Wigner functions. The functions used in this paper are related to the Wigner functions by a phase

$$p_l^{m\mu}(\theta) = d_{m\mu}^l(\theta)\exp\left\{\mathrm{i}\frac{\pi}{2}(\mu - m)\right\}. \tag{72}$$

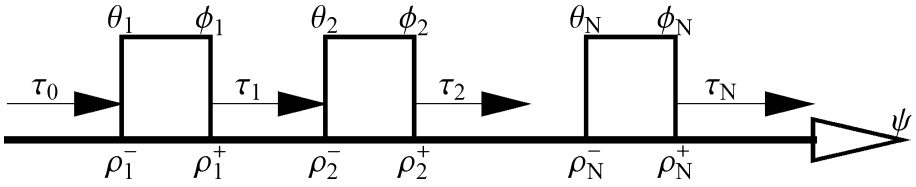

Fig. 1. Schematic representation of a N-pulse NMR experiment.

2.6. NMR algebraic description

A general NMR experiment is realized as the repetition of the excitation–acquisition cycle schematically depicted in Fig. 1. The excitation consists of a sequence of hard pulses $\mathbf{P}_1,\ldots,\mathbf{P}_N$, with flip angles θ_k, phases ϕ_k followed by delays τ_k. The initial delay, τ_0, is considered to be measured from the last excitation of the previous sequence. Measurements are performed at times τ_N; whenever the time t is mentioned, the equality $t=\tau_N$ is understood.

Denoting the density matrices before and after the kth pulse as ρ_k^- and ρ_k^+, the evolution of the density matrix during the experiment is given by the chain of equations

$$\begin{aligned}&|\rho_k^-\rangle\rangle=\widetilde{\mathbf{U}}_\delta(\tau_{k-1})\bullet|\rho_{k-1}^+\rangle\rangle=\mathbf{U}_\delta(\tau_{k-1})|\rho_{k-1}^+\rangle\rangle+|\rho_{\mathrm{rec}}(\tau_{k-1})\rangle\rangle,\\&|\rho_k^+\rangle\rangle=\mathbf{P}_k(\theta_k,\phi_k)|\rho_k^-\rangle\rangle.\end{aligned}\tag{73}$$

As long as the inter sequence separation (i.e., τ_0) is considered long compared with the relaxation times, the starting point of the previous recurrence is given by the equilibrium density matrix (the memory of the previous excitations is lost)

$$|\rho_1^-\rangle\rangle=|\rho_{\mathrm{rec}}(\tau_0)\rangle\rangle\approx|10\rangle\rangle.\tag{74}$$

The measured signal is the average of the transverse magnetization, up to a receiver phase ψ. For perfect quadrature detection, this is expressed as

$$\mathrm{e}^{\mathrm{i}\psi}\widetilde{S}_\delta(\vec{\theta},\vec{\phi},\vec{\tau})=\mathrm{e}^{\mathrm{i}\psi}\langle\langle 11|\rho(\tau_N)\rangle\rangle\tag{75}$$

and corresponds to the superspace matrix element

$$\begin{aligned}\widetilde{S}_\delta(\vec{\theta},\vec{\phi},\vec{\tau})=\langle\langle 11|\widetilde{\mathbf{U}}_\delta(\tau_N)\bullet\mathbf{P}_N\widetilde{\mathbf{U}}_\delta\\\bullet(\tau_{N-1})\mathbf{P}_{N-1}\ldots\widetilde{\mathbf{U}}_\delta(\tau_1)\\\bullet\mathbf{P}_1|\rho_{\mathrm{rec}}(\tau_0)\rangle\rangle.\end{aligned}\tag{76}$$

Taking in to consideration Eq. (73), the last expression transforms in a sum of N terms, comprising a main ($K=0$) and $N-1$ residual signals ($K\neq 0$)

$$\mathrm{e}^{\mathrm{i}\psi}\widetilde{S}_\delta(\vec{\theta},\vec{\phi},\vec{\tau})=\sum_{K=0}^{N-1}\mathrm{e}^{\mathrm{i}\psi}S_\delta^{(K)}(\vec{\theta},\vec{\phi},\vec{\tau}),\tag{77}$$

where each of the sub-signals is expressed as matrix elements of a product of linear operators

$$\begin{aligned}S_\delta^{(K)}(\vec{\theta},\vec{\phi},\vec{\tau})=\langle\langle 11|\mathbf{U}_\delta(\tau_N)\mathbf{P}_N(\theta_N,\phi_N)\ldots\mathbf{U}_\delta(\tau_{K+1})\\\times\mathbf{P}_{K+1}(\theta_{K+1},\phi_{K+1})|\rho_{\mathrm{rec}}(\tau_K)\rangle\rangle.\end{aligned}\tag{78}$$

The property of the Kth residual to have no dependence of the first K pulses, makes it possible to design a filtering scheme in which all residual contributions are canceled. This class of filtered experiments, named 'T_2 experiments' is described in this paper, and it will be explicitly characterized at the end of this section. For T_2 experiments, after filtering, the non-vanishing contribution comes from the main signal, only, and the relation

$$\begin{aligned}S_\delta(\vec{\theta},\vec{\phi},\vec{\tau})\underset{\mathrm{AF}}{=}S_\delta^{(0)}(\vec{\theta},\vec{\phi},\vec{\tau})=\langle\langle 11|\mathbf{U}_\delta(\tau_N)\\\times\mathbf{P}_N(\theta_N,\phi_N)\ldots\mathbf{U}_\delta(\tau_1)\mathbf{P}_1(\theta_1,\phi_1)|10\rangle\rangle\end{aligned}\tag{79}$$

has the meaning that the equality holds *after* a proper *filtering*.

The effect of the off-resonance irradiation can be absorbed into the RF pulse phases. The property

$$\begin{aligned}\mathrm{e}^{-\mathrm{i}\delta\tau\mathbf{J}_Z}\mathbf{P}(\theta,\phi)&=\mathrm{e}^{-\mathrm{i}\delta\tau\mathbf{J}_Z}\mathrm{e}^{-\mathrm{i}\phi\mathbf{J}_Z}\mathbf{P}(\theta,0)\mathrm{e}^{\mathrm{i}\phi\mathbf{J}_Z}\\&=\mathbf{P}(\theta,\varphi+\delta\tau)\mathrm{e}^{-\mathrm{i}\delta\tau\mathbf{J}_Z}\end{aligned}\tag{80}$$

brings any of the matrix elements in Eq. (78) in the equivalent form

$$\begin{aligned}&\langle\langle 11|\mathbf{U}_\delta(\tau_N)\mathbf{P}_N(\theta_N,\phi_N)\ldots\mathbf{U}_\delta(\tau_k)\mathbf{P}_k(\theta_k,\phi_k)|\rho_{\mathrm{rec}}(\tau_{K-1})\rangle\rangle\\&\quad=\langle\langle 11|\mathbf{U}(\tau_N)\mathbf{P}_N(\theta_N,\phi_N^\delta)\ldots\mathbf{U}(\tau_k)\mathbf{P}_k(\theta_k,\phi_k^\delta)\\&\qquad\times\exp(-\mathrm{i}\delta(\tau_N+\ldots+\tau_k)\mathbf{J}_Z)|\rho_{\mathrm{rec}}(\tau_{K-1})\rangle\rangle\end{aligned}\tag{81}$$

with the distorted phases defined by

$$\phi_m^\delta=\phi_m+\delta(\tau_N+\tau_{N-1}+\ldots+\tau_m).\tag{82}$$

The density matrix at the right-hand side of Eq. (81) is longitudinal, therefore

$$\mathrm{e}^{-\mathrm{i}\alpha\mathbf{J}_Z}|\rho_{\mathrm{rec}}(\tau)\rangle\rangle=|\rho_{\mathrm{rec}}(\tau)\rangle\rangle.\tag{83}$$

Finally, the off resonance signal is equivalent with the on resonance signal with distorted phases

$$\mathrm{e}^{\mathrm{i}\psi}S_\delta(\vec{\theta},\vec{\phi},\vec{\tau})=\mathrm{e}^{\mathrm{i}\psi}S(\vec{\theta},\vec{\phi}^{\,\delta},\vec{\tau}).\tag{84}$$

The reverse is also true, once the on resonance signal as a function of the phases is known, the off resonance signal is obtained redefining the RF phases according to Eq. (82).

The explicit dependence of the matrix element $S(\vec{\theta},\vec{\phi},\vec{\tau})$ on the RF phases is a prerequisite for phase cycling design and it is obtained using the $|lm\rangle\rangle$ basis. In

terms of projectors over subspaces with given quantum magnetic numbers m, $\mathbf{M}_m = \sum_{l=|m|}^{3} |lm\rangle\rangle\langle\langle lm|$, the propagators and hard pulses can be rewritten as

$$\begin{aligned}\mathbf{U}(t) &= \sum_m \mathbf{U}(t)\mathbf{M}_m,\\ \mathbf{P}(\theta,\phi) &= \sum_{m,\mu} \mathrm{e}^{\mathrm{i}\phi(\mu-m)}\mathbf{M}_m\mathbf{P}(\theta)\mathbf{M}_\mu.\end{aligned} \tag{85}$$

Using this decomposition, the signal is given by the sum over intermediate magnetic numbers

$$\mathrm{e}^{\mathrm{i}\psi}S_\delta(\vec{\theta},\vec{\phi},\vec{\tau}) = \sum_{\vec{m}} \mathrm{e}^{\mathrm{i}\psi}\mathrm{e}^{-\mathrm{i}\vec{\xi}\vec{\phi}}\mathrm{e}^{-\mathrm{i}\delta\vec{m}\vec{\tau}}A_{\vec{m}}(\vec{\theta},\vec{\tau}) \tag{86}$$

with the auxiliary quantities, the "coherence-transfer pathway" vector $\vec{\xi}$ [18] and the "pathway vector" $\vec{m}$ [19] given by

$$\begin{aligned}\vec{\xi} &= (m_1, m_2 - m_1, \ldots, m_{N-1} - m_{N-2}, 1 - m_{N-1}),\\ \vec{m} &= (\,m_1 \quad m_2 \quad \ldots \quad m_{N-1} \quad m_N\,).\end{aligned} \tag{87}$$

The summation in Eq. (86) is restricted at both ends, $m_1 = -1, 0, 1$ and $\mathrm{m}_N = 1$, therefore there are $3\times 7^{N-2}$ distinct terms in summation for $N \geqslant 2$, and a single term for $N = 1$. For T_2 experiments, due to the restrictions $m_1 = -1, 1$ and $m_i \neq 0$, only $2\times 6^{N-2}$ terms survive

$$\mathrm{e}^{\mathrm{i}\psi}S_\delta(\vec{\theta},\vec{\phi},\vec{\tau}) \underset{\mathrm{AF}}{=} \sum_{m_1=-1}^{1}\sum_{m_2,\ldots m_{N-1}=-3}^{3} \mathrm{e}^{\mathrm{i}\psi}\mathrm{e}^{-\mathrm{i}\vec{\xi}\vec{\phi}}\mathrm{e}^{-\mathrm{i}\delta\vec{m}\vec{\tau}}A_{\vec{m}}(\vec{\theta},\vec{\tau})\Big|_{m_N=1, m_i\neq 0}. \tag{88}$$

The complex amplitudes

$$A_{\vec{m}} = \langle\langle 11|\mathbf{M}_{m_N}\mathbf{U}(\tau_N)\mathbf{M}_{m_N}\mathbf{P}(\theta_N)\ldots\mathbf{M}_{m_1}\mathbf{U}(\tau_1)\mathbf{M}_{m_1}\mathbf{P}(\theta_1)|10\rangle\rangle \tag{89}$$

can be further expressed in terms of propagator and hard pulse matrix elements

$$\begin{aligned}A_{\vec{m}} = \sum_{l_{N-1}=|m_{N-1}|}^{3} \cdots \sum_{l_2=|m_2|}^{3} & u^{m_N}_{l_N l_{N-1}}(\tau_N)p^{m_N m_{N-1}}_{l_{N-1}}(\theta_N)\ldots u^{m_2}_{l_2 l_1}(\tau_2)\\ & \times p^{m_2 m_1}_{l_1}(\theta_2)u^{m_1}_{l_1 l_0}(\tau_1)p^{m_1 m_0}_{l_0}(\theta_1)\end{aligned} \tag{90}$$

with the constraints $l_N = 1$, $m_N = 1$, $m_0 = 0$. In a compact notation

$$\mathrm{e}^{\mathrm{i}\psi}S_\delta(\vec{\theta},\vec{\phi},\vec{\tau}) \underset{\mathrm{AF}}{=} \sum_{\vec{m}} \mathrm{e}^{\mathrm{i}\psi}\mathrm{e}^{-\mathrm{i}\vec{\xi}\vec{\phi}}\mathrm{e}^{-\mathrm{i}\delta\vec{m}\vec{\tau}} \sum_{\vec{l}>\vec{m}} U^{\vec{m}}_{\vec{l},1}(\vec{\tau})P^{\vec{m},0}_{\vec{l},1}(\vec{\theta}), \tag{91}$$

where the following products of matrix elements are defined

$$\begin{aligned}U^{\vec{m}}_{\vec{l},\lambda}(\vec{\tau}) &= \prod_{\alpha=1}^{N} u^{m_\alpha}_{l_\alpha l_{\alpha-1}}(\tau_\alpha), \quad l_0 = \lambda\\ P^{\vec{m},\mu}_{\vec{l},\lambda}(\vec{\theta}) &= \prod_{\alpha=1}^{N} p^{m_\alpha m_{\alpha-1}}_{l_{\alpha-1}}(\theta_\alpha), \quad l_0 = \lambda, \mathrm{m}_0 = \mu\end{aligned} \tag{92}$$

and the inequality $\vec{l} \geqslant \vec{m}$ is understood as $l \geqslant |m_i|$, for each $i = 1, \cdots, N$. When there is no possibility of confusion, the short forms are used

$$\begin{aligned}U^{m_1\cdots m_{N-1}}_{l_1\cdots l_{N-1}} &\equiv U^{\vec{m}}_{\vec{l},1}(\vec{\tau}) \equiv U^{\vec{m}}_{\vec{l}},\\ P^{m_1\cdots m_{N-1}}_{l_1\cdots l_{N-1}} &\equiv P^{\vec{m},0}_{\vec{l},1}(\vec{\theta}) \equiv P^{\vec{m}}_{\vec{l}}.\end{aligned} \tag{93}$$

The advantage of this formalism resides in the fact that it automatically generates the coherence pathways in a form suitable for symbolic calculation. The study of various filtering schemes can be realized without explicit calculation of the amplitudes. The form of Eq. (91) spells clearly the maximum amount of information that can be extracted from such NMR experiments.

The phase cycling filtering of the signal is performed by averaging the signal N_F times, over pulses phases, ϕ, and receiver phases, ψ. The filtered signal (denoted with superscript F) is the sum

$$S^\mathrm{F} = \frac{1}{N_\mathrm{F}}\sum_{\vec{\phi},\psi}\left\{\mathrm{e}^{\mathrm{i}\psi}S_\delta(\vec{\theta},\vec{\phi},\vec{\tau})\right\}. \tag{94}$$

By applying the summation on the coherence pathways representation, and by performing the sum over phases first, the signal takes a form similar to the original Eq. (86)

$$S^\mathrm{F} = \sum_{\vec{m}} A_{\vec{m}}(\vec{\theta},\vec{\tau})f_{\vec{m}}\mathrm{e}^{-\mathrm{i}\delta\vec{m}\vec{\tau}} \tag{95}$$

with a filtering-scheme-dependent coefficient

$$f_{\vec{m}} \equiv \frac{1}{N_\mathrm{F}}\sum_{\vec{\phi},\psi}\mathrm{e}^{\mathrm{i}(\psi-\vec{\xi}\vec{\phi})}. \tag{96}$$

The contribution of a given pathway $\vec{m}$ is canceled by the filtering provided that $f_{\vec{m}} = 0$. Using the results above, the class of T_2 experiments can be properly defined. A T_2 *experiment* is a filtered experiment in which $f_{\vec{m}}$ vanishes whenever an intermediate m_i is zero.

The connection with the NMR experiments requires, as a supplementary step, spatial averaging (denoted $\langle\rangle$), over a distribution of both offset values and flip angles. For simplicity, it is assumed that the distribution of flip angles is independent of the off resonance distribution. The averages, denoted $\langle\rangle_\theta$ and $\langle\rangle_\delta$ can then be performed separately bringing the measured signal to the form

$$\begin{aligned}\langle S^\mathrm{F}(t)\rangle &= \sum_{\vec{m}} f_{\vec{m}}\langle\mathrm{e}^{-\mathrm{i}\delta\vec{m}\vec{\tau}}\rangle_\delta\langle A_{\vec{m}}(\vec{\theta},\vec{\tau})\rangle_\theta\\ &= \sum_{\vec{m}} f_{\vec{m}}\langle\mathrm{e}^{-\mathrm{i}\delta\vec{m}\vec{\tau}}\rangle_\delta\sum_{\vec{l}\geqslant\vec{m}}\left\langle P^{\vec{m}}_{\vec{l}}(\vec{\theta})\right\rangle_\theta U^{\vec{m}}_{\vec{l}}(\vec{\tau}).\end{aligned} \tag{97}$$

Note that because the distribution of inhomogeneities is unknown, the averages $\langle P^{\vec{m}}_{\vec{l}}(\vec{\theta})\rangle_\theta$ as well as $\langle\mathrm{e}^{-\mathrm{i}\delta\vec{m}\vec{\tau}}\rangle_\delta$ are also unknown, which renders the direct fit of Eq. (97) unreliable for the purpose of determining physical properties of the system. Further implications of this observation are discussed below.

A component, $\vec{m}$, and its associated pathway, is called "echo-like" if the quantity

$$t_0 = -(m_1\tau_1 + \cdots + m_{N-1}\tau_{N-1}) \geqslant 0. \tag{98}$$

For echo-like components, the off-resonance dependent factor becomes exactly one at the time $\tau_N = t_0$ during the measurement period. Provided that a filtering scheme can be designed to select such a component, $\vec{m}$, the direct, non-B_0 biased, determination of the quantity

$$\langle A_{\vec{m}}(\vec{\theta},\vec{\tau})\rangle_\theta = \sum_{\vec{l}>\vec{m}} \left\langle P_{\vec{l}}^{\vec{m}}(\vec{\theta})\right\rangle_\theta U_{\vec{l}}^{\vec{m}}(\vec{\tau}) \tag{99}$$

is attainable, by performing a multidimensional experiment. By contrast, for the non-echo components, any measurement is biased by the effect of the B_0 inhomogeneities. Due to B_1 inhomogeneities the averages $\langle P_{\vec{l}}^{\vec{m}}(\vec{\theta})\rangle_\theta$ are unknown, independent quantities rendering the direct fit of Eq. (99) unreliable, unless a factorization of the flip angle dependent terms is possible.

Two strategies are possible for experimentally measuring the matrix elements $U_{\vec{l}}^{\vec{m}}(\vec{\tau})$, namely, the "variable echo" and "fixed echo" time strategies. In the "variable echo" time strategy, only one, echo-like, coherence pathway is selected. By simultaneously varying the pulse delays, the quantity $U_{\vec{l}}^{\vec{m}}(\vec{\tau})$ is measured for $\vec{m}\vec{\tau} = 0$, up to a multiplicative constant. One of the cases in which the selection of a single coherence pathway is possible is given by maximally quantum-filtered signals, when only the coherences with extreme values of magnetic numbers survive

$$|m_1| = 1, \quad |m_2| =, \ldots, = |m_{N-1}| = 3, \quad m_N = 1. \tag{100}$$

The "fixed echo" time strategy is based on the condition that the position of the echo is constant

$$\tau_E \equiv \sum_{k=1}^{N-1} m_k \tau_k = \text{const.} \tag{101}$$

The signal acquired is proportional with the expression

$$S^{\mathrm{F}}(t) \approx u_{10}^{m_1}(\tau_1)\ldots u_{l_{N-1}l_{N-2}}^{m_{N-1}}(\tau_{N-1})u_{l_N l_{N-1}}^{m_N}(t)\langle \mathrm{e}^{\mathrm{i}\delta(t-\tau_E)}\rangle_\delta \tag{102}$$

from where the following non-biased expression is obtained

$$\int_{t_1}^{t_2} w(t)S^F(t)\,\mathrm{d}t \approx u_{10}^{m_1}(\tau_1)\ldots u_{l_{N-1}l_{N-2}}^{m_{N-1}}(\tau_{N-1}). \tag{103}$$

While the specific choice of the windowing function, $w(t)$, is not important from the point of view of the information provided by the experiment, it may affect the SNR of the experiment.

From the SNR point of view it is more convenient to acquire many components (echo and non-echo) together, therefore in the sum given by Eq. (97) destructive interference between various components occurs. In some special cases, as long as the cancellation is not severe, and the B_0 distribution can be estimated, this effect can be corrected at the data processing stage.

3. Theoretical results

3.1. One pulse experiment

The one pulse experiment, presented schematically in Fig. 2, is often used in NMR for calibrating the 90° pulse. The signal measured is given, in the infinite repetition time limit, by

$$\begin{aligned} S_\delta(\theta_1,\phi_1,\psi,t) &= \mathrm{e}^{\mathrm{i}\psi}\langle\langle 11|\mathbf{U}_\delta(t)\mathbf{P}(\theta_1,\phi_1)|10\rangle\rangle \\ &= \mathrm{e}^{\mathrm{i}(\psi-\phi_1-\delta t)}u_{11}^1(t)p_1^{10}(\theta). \end{aligned} \tag{104}$$

The filtering scheme, based on addition-subtraction with $\phi_1 = k\pi, \psi = k\pi, k = 0, 1$ (used to avoid DC baselines in the collected FID) produces the signal

$$S_\delta^{\mathrm{F}}(\theta,t) = \mathrm{e}^{-\mathrm{i}\delta t}u_{11}^1(t)p_1^{10}(\theta) = \frac{\mathrm{i}}{\sqrt{2}}\mathrm{e}^{-\mathrm{i}\delta t}u_{11}^1(t)\sin\theta. \tag{105}$$

After the average over B_0 and B_1 fields is taken

$$S_{\mathrm{macro}}(t) = \langle \mathrm{e}^{-\mathrm{i}\delta t}u_{11}^1(t)p_1^{10}(\theta)\rangle_{\delta,\theta} \approx \langle \mathrm{e}^{-\mathrm{i}\delta t}\rangle_\delta u_{11}^1(t)\langle\sin\theta\rangle_\theta. \tag{106}$$

The general form of the matrix element $u_{11}^1(t)$ is given in Appendix A.2.

The presence of the time dependent term $\langle \mathrm{e}^{-\mathrm{i}\delta t}\rangle_\delta$ makes the direct fit of the FID in Eq. (106) unreliable for the estimation of the actual relaxation rates, unless special precautions are taken in preparing the sample. Nevertheless, variations of the one pulse experiment can be used to experimentally estimate the (in)homogeneity of the B_1 field (the acquisition of a pulse width array [20]).

3.2. Two pulse experiment

The schematic representation of a two-pulse NMR experiment is presented in Fig. 3. One of the most useful and non-trivial, applications of this generic pulse-ac-

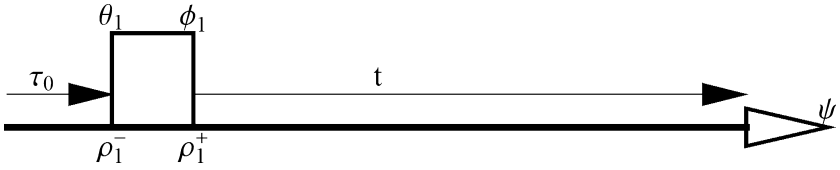

Fig. 2. Schematic representation of the one-pulse NMR experiment. A hard pulse of flip angle θ and phase ϕ is applied followed by data collection at time t.

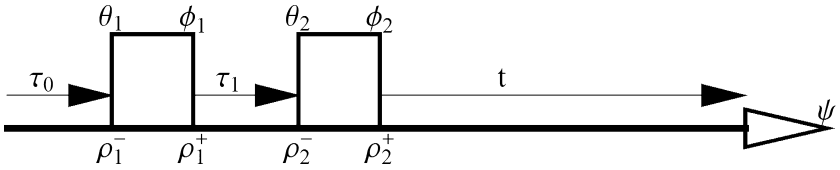

Fig. 3. Schematic representation of the two-pulse NMR experiment. A hard pulse, with flip angle θ_2 and phase ϕ_2 is applied τ_1 seconds after an initial pulse of flip angle θ_1 and phase ϕ_1. Data collection takes place at time t.

quire structure is the description of a spin echo experiment.

For a given separation τ_1 between the pulses, the measured signal at time $t = \tau_2$ is given by

$$e^{i\psi}S_\delta(\theta_1,\theta_2,\phi_1,\phi_2,\tau_1,t) = e^{i\psi}\langle\langle 11|\mathbf{U}_\delta(t)\mathbf{P}(\theta_2,\phi_2) \times \mathbf{U}_\delta(\tau_1)\mathbf{P}(\theta_1,\phi_1)|10\rangle\rangle. \quad (107)$$

In general, there are three distinct components: echo, residual, and non-echo ($m_1 = -1, 0, 1$, respectively)

$$e^{i\psi}S_\delta = e^{i\psi - i\delta t}(e^{-i(2\phi_2-\phi_1)+i\delta\tau_1}A_{-1} + e^{-i\phi_2}A_0 + e^{-i\phi_1 - i\delta\tau_1}A_1), \quad (108)$$

where

$$A_m(\theta_1,\theta_2,\tau_1,t) = \sum_{l=1}^{3} u_{l1}^1(t)u_{l1}^m(\tau_1)p_l^{1m}(\theta_2)p_1^{0m}(\theta_1). \quad (109)$$

To cancel the residual components (i.e., to obtain a T_2 experiment) using phase-cycling, the following condition has to be fulfilled

$$\sum_{\phi_2,\psi} e^{i(\psi-\phi_2)} = 0. \quad (110)$$

The pure echo component can thus be selected with a four phase scheme, satisfying the condition above, namely

$$\phi_1 = -k\pi/2, \quad \phi_2 = 0, \quad \psi = k\pi/2, \quad k = 0,1,2,3. \quad (111)$$

After averaging over flip angles (to account for spatial inhomogeneities in the B_1 field) and B_0 inhomogeneities the macroscopic signal becomes

$$S_{\text{macro}}^{\text{F},-1}(\theta_1,\theta_2,\tau_1,t) = \langle e^{-i\delta(t-\tau_1)}\rangle_\delta \langle A_{-1}(\theta_1,\theta_2,\tau_1,t)\rangle_\theta. \quad (112)$$

Making use of the propagator property $\mathbf{U}(t+\tau_1) = \mathbf{U}(t)\mathbf{U}(\tau_1)$, together with the symmetry relation $u_{lk}^{-m} = (-)^{l+k}u_{lk}^m$ the sum-of-times matrix element

$$u_{11}^1(t+\tau_1) = u_{11}^1(t)u_{11}^{-1}(\tau_1) - u_{21}^1(t)u_{21}^{-1}(\tau_1) + u_{31}^1(t)u_{31}^{-1}(\tau_1) \quad (113)$$

can be formed, and the amplitude of the echo component takes the form

$$i\sqrt{2}A_{-1} = \sin\theta_1\left(\sin^2\frac{\theta_2}{2}u_{11}^1(t+\tau_1) - \sin^2\theta_2 u_{21}^1(t)u_{21}^1(\tau_1) - \frac{5}{8}\sin^2\theta_2(1-3\cos\theta_2)u_{31}^1(t)u_{31}^1(\tau_1)\right). \quad (114)$$

In particular, when the B_1 field is homogeneous the flip angle can be ideally calibrated, the condition $\theta_1 = \pi/2$, $\theta_2 = \pi$ is then easily realized leading to the following expression for the measured signal

$$S_{\text{macro}}^{\text{F},-1}\left(\frac{\pi}{2},\pi,\tau_1,t\right) = \langle e^{-i\delta(t-\tau_1)}\rangle_\delta u_{11}^1(t+\tau_1). \quad (115)$$

In this ideal case, it is possible to extract the function $u_{11}^1(2t)$ by a 2D experiment in which the delay between pulses, τ_1, is varied and the measurement takes place at the time $t = \tau_1$. In the general case, when the B_1 is not uniform across the sample volume, the quantity determined by the 2D experiment is the more complex $\langle A_{-1}(\theta_1,\theta_2,t,t)\rangle_\theta$

$$\langle A_{-1}(\theta_1,\theta_2,t,t)\rangle_\theta = \left\langle \sin\theta_1\sin^2\frac{\theta_2}{2}\right\rangle_\theta u_{11}^1(2t) - \langle\sin\theta_1\sin^2\theta_2\rangle_\theta u_{21}^1(t)u_{21}^1(t) - \frac{5}{8}\langle\sin\theta_1\sin^2\theta_2 (1-3\cos\theta_2)\rangle_\theta u_{31}^1(t)u_{31}^1(t). \quad (116)$$

For liquids, the identities $u_{21}^1 = u_{31}^1 = 0$ ensure the determination of $u_{11}^1(2t)$ even under non-ideal conditions

$$S_{\text{macro,liquids}}^{\text{F},-1}(\theta_1,\theta_2,t,t) \approx \left\langle \sin\theta_1\sin^2\frac{\theta_2}{2}\right\rangle_\theta u_{11}^1(2t). \quad (117)$$

In the general case, the flip angle dependent contributions from u_{21}^1 and u_{31}^1 terms make the direct extraction of u_{11}^1 in the presence of B_1 inhomogeneities impossible. Under such conditions, the extraction of physical parameters (relaxation rates) becomes unreliable. A similar conclusion has already been reached by Brown and Wimperis [21]. In Brown's report, however, the unstable nature of a non-linear fit to a sum of three exponentials was described as the leading reason for the unsuitability of a two-pulse and acquire experiment as a mean to measure relaxation rates. Our analysis here indicates that even if the fit was to be accurate, the biased nature of the 90°–180° experiment in the presence of B_1 inhomogeneities makes the estimation of relaxation rates unreliable.

As a further example, we consider the case in which the static quadrupolar interaction is absent. Under such conditions, the Hahn echo experiment produces a signal, which, at measurement time t is proportional to

$$A_{-1}^{\mathrm{H}} = \left\langle \sin\theta_1 \sin^2\frac{\theta_2}{2} \right\rangle_\theta \left(\frac{3}{5}f^2 + \frac{2}{5}s^2\right) - \frac{5}{8}\langle \sin\theta_1 \sin^2\theta_2 (1 - 3\cos 2\theta_2)\rangle_\theta \left(\frac{\sqrt{6}}{5}f - \frac{\sqrt{6}}{5}s\right)^2. \quad (118)$$

For this signal, the five parameter function

$$a\frac{1}{5}(3\mathrm{e}^{-2t/T_f} + 2\mathrm{e}^{-2t/T_s}) - b\frac{6}{25}(\mathrm{e}^{-t/T_s} - \mathrm{e}^{-t/T_f})^2 + c \quad (119)$$

is the natural choice for the extraction of the relaxation parameters with the amplitudes given by:

$$a = \left\langle \sin\theta_1 \sin^2\frac{\theta_2}{2} \right\rangle_\theta, \qquad b = \frac{5}{8}\langle \sin\theta_1 \sin^2\theta_2 (1 - 3\cos 2\theta_2)\rangle_\theta. \quad (120)$$

In the ideal situation of both perfect calibration and B_1 homogeneous field $b = 0$. Note, however, that in the presence of B_1 inhomogeneities the calibration of the 180° pulse only guarantees that $\langle \sin\theta_2\rangle_\theta = 0$ and the quantity $\frac{5}{8}\langle \sin\theta_1 \sin^2\theta_2 (1 - 3\cos 2\theta_2)\rangle_\theta$ could be still non-zero. A fit to the first term of Eq. (119) (the standard bi-exponential form used in the literature) will still be biased leading to a poor determination of the underlying relaxation rates. The bias, reflected by the presence of the b-term, depends on the B_1 distribution in the sample, which depends in turn on the shape of the sample and coil-sample geometry. As a result of the strong correlation between the parameters obtained by non-linear fit, the relaxation times are themselves biased.

3.3. Three pulse experiment

Using the diagram in Fig. 4, we have that the relevant matrix element giving the signal at time $t = \tau_3$, reads

$$\mathrm{e}^{\mathrm{i}\psi} S_\delta(\vec{\theta}, \vec{\phi}, \vec{\tau}) = \mathrm{e}^{\mathrm{i}\psi}\langle\langle 11|\mathbf{U}(\tau_3)\mathbf{P}_3\mathbf{U}(\tau_2)\mathbf{P}_2\mathbf{U}(\tau_1)\mathbf{P}_1|10\rangle\rangle \quad (121)$$

from where the decomposition in terms of coherences reads

$$\mathrm{e}^{\mathrm{i}\psi} S_\delta(\vec{\theta}, \vec{\phi}, \vec{\tau}) = \sum_{m_1=-1}^{1}\sum_{m_2=-3}^{3} \mathrm{e}^{\mathrm{i}\psi}\mathrm{e}^{-\mathrm{i}(m_1\phi_1 + m_2(\phi_2-\phi_1)+(\phi_3-\phi_2))} \times \mathrm{e}^{-\mathrm{i}\delta(m_1\tau_1 + m_2\tau_2 + \tau_3)} A_{m_1 m_2}(\vec{\theta}, \vec{\tau}) \quad (122)$$

with the individual amplitudes having the explicit form (90)

$$A_{m_1 m_2} = \sum_{l_\alpha = |m_\alpha|}^{3} u_{1 l_2}^{1}(\tau_3) u_{l_2 l_1}^{m_2}(\tau_2) u_{l_1 1}^{m_1}(\tau_1) p_{l_2}^{1 m_2}(\theta_3) p_{l_1}^{m_2 m_1}(\theta_2) p_1^{m_1 0}(\theta_1) = \sum_{l_\alpha = |m_\alpha|}^{3} U_{l_1 l_2}^{m_1 m_2} P_{l_1 l_2}^{m_1 m_2}. \quad (123)$$

The classification for the terms occurring in Eq. (122) is straightforward. For a T_2 experiment, there are twelve terms, from which, as a general rule, six are echo like. There are exceptional situations when $\tau_2 \approx k\tau_1/2$, $k = 0, 1, \ldots, 6$. When the condition $\tau_2 < \tau_1/3$ is fulfilled, the six echoes are located at

$$\tau_3^{\mathrm{e}}(m_2) = \tau_1 - m_2\tau_2, \quad m_2 = -3, \ldots 3, \quad m_2 \neq 0 \quad (124)$$

Even though the effect of the last two successive RF pulses is equivalent to that of a single RF pulse, the additional freedom to manipulate the relative phase between them allows the selection of a given m_2 order, therefore, reducing the number of matrix element products $u_{l1}^{1} u_{l1}^{m}$ entering in the summation in Eq. (123).

By selecting only the coherence pathways with $m_2 = \pm 3$ (named here "total TQ filtering"), the corresponding amplitudes are completely factored

$$A_{m_1=\pm1, m_2=\pm3}(\vec{\theta}, \vec{\tau}) = P_{33}^{m_1 m_2}(\vec{\theta}) U_{33}^{13}(\vec{\tau}) = P_{33}^{m_1 m_2}(\vec{\theta}) u_{31}^{1}(\tau_1) u_{33}^{3}(\tau_2) u_{31}^{1}(\tau_3). \quad (125)$$

The relevant, flip angle dependent, coefficients, organized in a matrix form for clarity, are given by

$$\begin{pmatrix} P_{33}^{-1,-3} \\ P_{33}^{-1,3} \\ P_{33}^{1,-3} \\ P_{33}^{1,3} \end{pmatrix} = \frac{15\mathrm{i}}{16\sqrt{2}} \sin\theta_1 \sin^2\theta_2 \sin^2\theta_3 \begin{pmatrix} -c_2 s_3 \\ -s_2 c_3 \\ c_2 c_3 \\ s_2 s_3 \end{pmatrix}$$

with $c_\alpha = \cos^2\frac{\theta_\alpha}{2}$, $s_\alpha = \sin^2\frac{\theta_\alpha}{2}$ (126)

When $\tau_2 < \tau_1/3$, only the components $(-1, \pm 3)$ give echoes, located at $\tau_3 = \tau_1 \mp 3\tau_2$. For $\tau_2 > \tau_1/3$ the echoes are given by the components $(-1, -3)$ and $(1, -3)$. In the most selective experiments, the individual components are isolated. This can be realized using cycling schemes with 10 phases

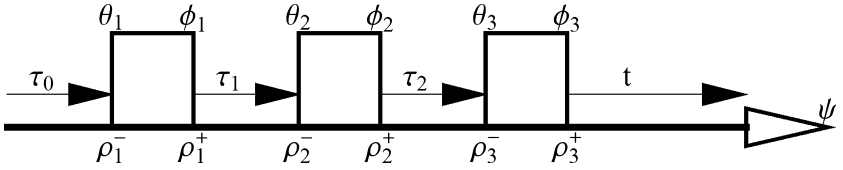

Fig. 4. Schematic representation of the three-pulse NMR experiment. A hard pulse, with flip angle θ_3 and phase ϕ_3 is applied τ_2 seconds after an initial two-pulse excitation has taken place (with flip angles θ_2 and θ_1 and phases ϕ_2 and ϕ_1, respectively). Data collection takes place at time t.

$$\phi_1 = \alpha_1 k\pi/5, \quad \phi_2 = \alpha_2 k\pi/5, \\ \phi_3 = \alpha_3 k\pi/5, \quad \psi = k\pi, \qquad k = 0,\ldots,9 \tag{127}$$

with the coefficients for each component given in the following table

	TQ^{-+}	TQ^{--}	TQ^{+-}	TQ^{++}
(m_1, m_2)	$(-1,+3)$	$(-1,-3)$	$(+1,-3)$	$(+1,+3)$
α_1	1	1	1	1
α_2	2	0	0	4
α_3	1	−2	1	7

(128)

The selection of both echo components is realized with the eighteen-phase scheme, TQ^-

$$\phi_1 = \frac{\pi}{9}k, \quad \phi_2 = \frac{2\pi}{9}k, \quad \phi_3 = -\frac{\pi}{9}k, \\ \psi = k\pi, \qquad k = 0,\ldots,17. \tag{129}$$

Finally, the simultaneous acquisition of all four TQ components is realized with the following composite twelve phases cycle TQ

$$\phi_1 = \frac{\pi}{3}k + \frac{\pi}{6}, \ \phi_2 = \frac{\pi}{3}k - \frac{\pi}{3}, \ \phi_3 = 0, \ \psi = k\pi, \quad k = 0,\ldots,5 \\ \phi_1 = \frac{\pi}{3}k + \frac{\pi}{6}, \ \phi_2 = \frac{\pi}{3}k - \frac{\pi}{3}, \ \phi_3 = 0, \ \psi = k\pi + \pi, \quad k = 6,\ldots,11. \tag{130}$$

The additional six phases, compared with [5], are introduced to obtain a T_2 experiment.

The experiments give the filtered signals, in which, for simplicity the factor $15/(16\sqrt{2})$ was dropped, and the notations $c_\alpha = \cos^2(\theta_\alpha/2)$, $s_\alpha = \sin^2(\theta_\alpha/2)$ introduced in Eq. (126) are used

$$S_\delta^{-1,3} = -\mathrm{i}e^{-\mathrm{i}\delta(\tau_3-\tau_1-3\tau_2)} U_{33}^{13}(\vec{\tau}) \sin\theta_1 \sin^2\theta_2 \sin^2\theta_3 s_2 c_3, \tag{131}$$

$$S_\delta^{-1,-3} = -\mathrm{i}e^{-\mathrm{i}\delta(\tau_3-\tau_1+3\tau_2)} U_{33}^{13}(\vec{\tau}) \sin\theta_1 \sin^2\theta_2 \sin^2\theta_3 c_2 s_3, \tag{132}$$

$$S_\delta^{-1,\pm 3} = -\mathrm{i}e^{-\mathrm{i}\delta(\tau_3-\tau_1)} U_{33}^{13}(\vec{\tau}) \sin\theta_1 \sin^2\theta_2 \sin^2\theta_3 \\ \times (e^{3\mathrm{i}\delta\tau_2} c_2 s_3 + e^{-3\mathrm{i}\delta\tau_2} s_2 c_3), \tag{133}$$

$$S_\delta^{\pm 1,\pm 3} = e^{-\mathrm{i}\delta\tau_3} U_{33}^{13}(\vec{\tau}) \sin\theta_1 \sin^2\theta_2 \sin^2\theta_3 \\ \times \{e^{+\mathrm{i}\delta\tau_1}[e^{-3\mathrm{i}\delta\tau_2} s_2 c_3 + e^{3\mathrm{i}\delta\tau_2} c_2 s_3] \\ + e^{-\mathrm{i}\delta\tau_1}[e^{-3\mathrm{i}\delta\tau_2} c_2 c_3 + e^{3\mathrm{i}\delta\tau_2} s_2 s_3]\}. \tag{134}$$

In the case in which all pulses are identical, $\theta_1 = \theta_2 = \theta_3 = \theta$, the signal simplifies to

$$S_\delta^{-1} = -\mathrm{i}e^{-\mathrm{i}\delta(\tau_3-\tau_1)} U_{33}^{13}(\vec{\tau}) \sin^7\theta \cos(3\mathrm{i}\delta\tau_2), \tag{135}$$

$$S_\delta^{TQ} = e^{-\mathrm{i}\delta\tau_3} U_{33}^{13}(\vec{\tau}) \sin^5\theta \times \{\cos\delta\tau_1 \cos 3\delta\tau_2 \\ - \cos\theta \sin\delta\tau_1 \sin 3\delta\tau_2 - \mathrm{i}\cos\theta(\cos\delta\tau_1 \\ \times \sin 3\delta\tau_2 + \cos\theta \sin\delta\tau_1 \cos 3\delta\tau_2)\}. \tag{136}$$

4. Methods and experimental results

Phantom experiments were performed to illustrate the used of the proposed approach for the theoretical description of NMR pulsed experiments. These experiments were designed to illustrate the bias in the relaxation parameters that could result from variations in the B_0 and B_1 field across the sample and how the proposed approach can help isolate these effects during the analysis of the signal (i.e., by identifying useful factorizations in the signal envelope). All experiments were performed on a vertical bore, 7 Tesla Bruker DMX300 spectrometer (Bruker AG, Germany). The phantoms consisted of agar gels, as such gels are known to exhibit bi-exponential relaxation behavior due to the isotropic slow motion experienced by the sodium ions in the agar environment.

To obtain a strong deuterium lock signal, the gel was prepared using D_2O instead of distilled water. All chemicals used (10 cc D_20, 0.2 g NaCl, 2 g agar powder) were acquired from Sigma–Aldrich, St. Louis, MO. The samples were prepared by bringing the mixture close to the boiling point while continuously mixing the NaCl and agar using a magnetic stirring plate and an uncovered Erlenmeyer flask. After mixing-in and dissolving the chemicals, the mixture was allowed to cool before being placed in 10 mm NMR tubes. The resulting samples (2) were cylindrical in shape (10 mm diameters) and of different lengths. The smallest sample, which had a height of 1 cm, was used to illustrate the effects of B_0 inhomogeneities. The other sample had a height of 4 cm and was used to illustrate the effects of B_1 inhomogeneities.

One-, two-, and three-pulse experiments were performed to verify the predictions of the model. The one-pulse experiment data were acquired on both samples, using the same pulse sequence program. Eight FIDs were added in each one-pulse experiment, using a phase cycling scheme with $\phi_1 = k\pi$, $\psi = k\pi$, $k = 0, 1$. Shimming was performed in two stages. First, the lock signal level was maximized by modifying the shim gradients. Second, a modification of the paropt utility shipped with the XWIN-NMR software suite was used to maximize the amplitude of the spectral peak, by varying the shim gradients, followed by acquisition and Fourier transformation of the signal. The sensitivity of this approach is better than the one based on the lock signal.

In Fig. 5, it is presented a comparison between the measured data (symbols) and the non-linear fit (solid line) for the small (bullets) and large (stars) agar phantoms. The results indicate that the small sample is characterized by larger B_0 inhomogeneities within the RF coil volume leading to an "artificial" shortening of the relaxation times.

To illustrate the effects of B_1 inhomogeneities across the sample, the one-pulse experiment was performed in a 2D fashion with the extra dimension being given by

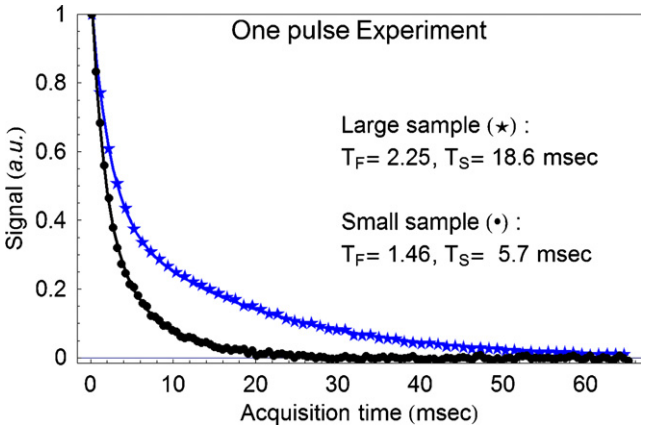

Fig. 5. FID and non-linear fit using the biexponential, a(6 exp($-t$/TFAST) + 4 exp($-t$/TSLOW)) + b, from a one pulse experiment on the small agar phantom (bullets) and the large agar phantom (stars). (TR = 191 ms, 8 averages).

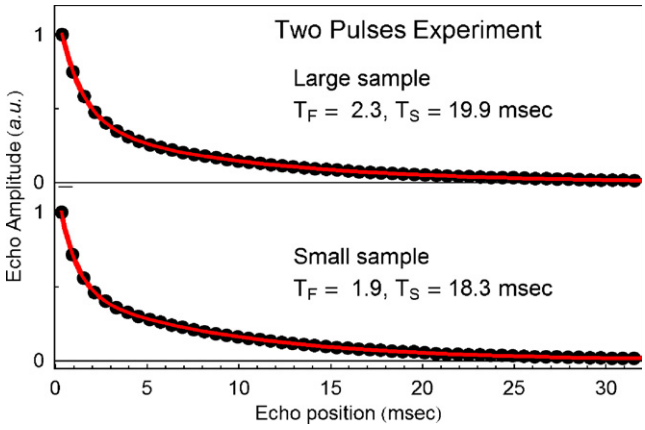

Fig. 7. Dependence of the NMR signal from a two pulse experiment on the inter-pulse separation for the small agar phantom (lower part) and large phantom (upper part). Each data point corresponds to the peak amplitude of the corresponding FID (TR = 209–285 ms, 8 averages). The solid line indicates the fit to the signal envelope using the three terms function of the inter-pulse separation t, a (15 exp($-2t$/TFAST) + 10 exp($-2t$/TSLOW)) − 6 b (exp($-t$/TFAST) − exp($-t$/TSLOW))^2 + c.

the pulse length [20]. Fig. 6, presents the integral of the measured data for the small (bullets) and large (stars) samples as a function of the pulse length (128 values between 10 and 518 μs). Clearly, larger B_1 inhomogeneities are present in the large agar sample, this conclusion being based on the higher degree of signal loss as the flip angle increases (increase in pulse length).

To illustrate the theoretical findings from the two-pulse theoretical model another set of measurements was performed. In these two-pulse experiments, the time delay between the pulses was increased from 0.3 to 38.4 ms (128 equal steps). Each individual FID was recorded with a time resolution of four microseconds and twenty-four points in the FID averaged to obtain an estimate of the FID intensity at the echo. This estimated peak FID value was graphed as a function of the inter-pulse delay for the small (Fig. 7, lower part) and large (Fig. 7, upper part) agar samples.

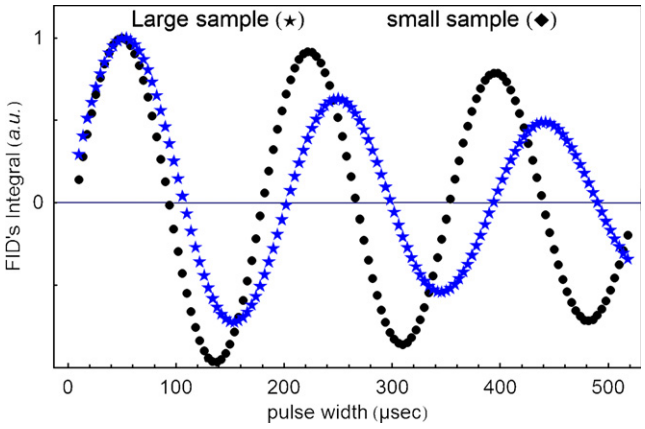

Fig. 6. Dependence of the NMR signal on the RF pulse length for the small (bullets) and the large (stars) sample. Each data point corresponds to the integral of the FID (TR = 191 ms, 16 averages) following the RF pulse with corresponding pulse width.

As expected, for the small sample the effect of B_1 inhomogeneities is largely removed. For the large sample, the quality of the data is not significantly enhanced. Note that from Eq. (120) above, one measure for the size of the B_1 inhomogeneities within the sample can be given by the ratio b/a, which can be obtained from the best fit to the function $a(3e^{-2t/T_F} + 2e^{-2t/T_S})/5 - b(e^{-t/T_S} - e^{-t/T_F})^2/25 + c$. For the small sample (homogeneous B_1) this ratio yields $b/a = 0.11$ while for the large sample (inhomogeneous B_1) $b/a = 0.34$.

The variable echo three-pulse experiment is demonstrated next using the ten phase cycle from Eq. (128). Choosing to select only the $(-1,-3)$ component, an echo is formed and a non-biased 2D experiment is possible. The preparation delay is varied between 0.2 and 51.2 ms, in 256 equidistant steps and twenty FIDs are averaged for each delay (the FIDs are acquired with a time resolution of 8 μs and 80 points are used in the estimation of the peak). The results of this experimental procedure are presented in Fig. 8 as the lower and upper parts of the plot, for the small and large agar samples, respectively. Taking in consideration that the echo forms at the measurement moment $t = \tau_1 + 3\tau_2$, the fitting function, as given by the Eq. (132), in the absence of static quadrupolar interaction is

$$\begin{aligned} f(t) &= a u^1_{31}(t - 3\tau_2) u^1_{31}(t) \\ &= a\left(\exp\left\{-\frac{t-3\tau_2}{T_S}\right\} - \exp\left\{-\frac{t-3\tau_2}{T_F}\right\}\right) \\ &\quad \times \left(\exp\left\{-\frac{t}{T_S}\right\} - \exp\left\{-\frac{t}{T_S}\right\}\right). \end{aligned}$$

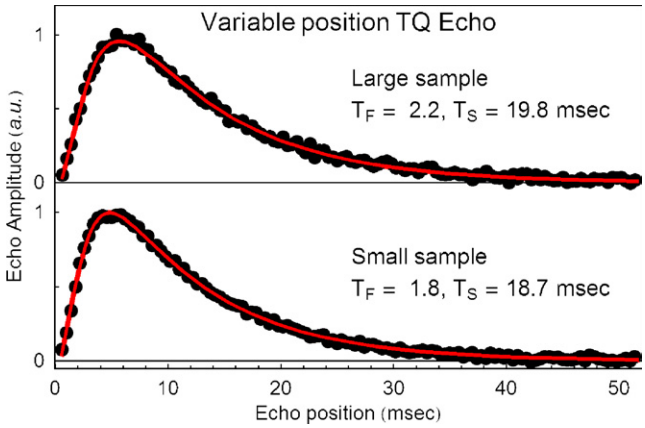

Fig. 8. Dependence of the NMR signal from a three pulse experiment on position of the echo (a function of the inter-pulse delay) for the small (lower part of the plot) and large (upper part of the plot) agar phantom. Each data point corresponds to the amplitude of the echo (TR = 157–259 ms, 20 averages). The solid line indicates the fit to the signal envelope, as described in text.

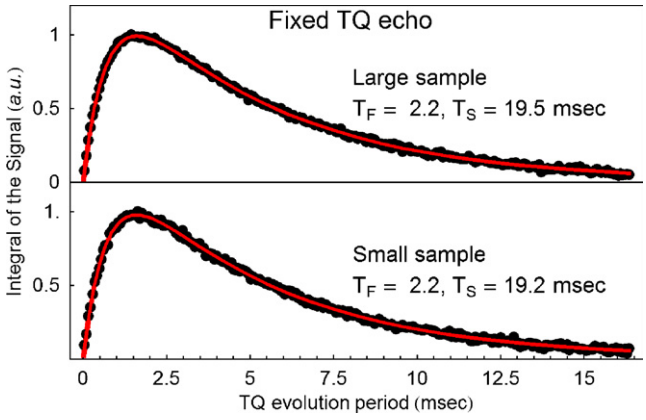

Fig. 9. Dependence of the integral of NMR signal from a three pulse experiment on the TQ evolution time, for the small agar phantom (lower part) and large agar phantom (upper part). Each data point corresponds to the time integral of the corresponding FID (TR = 217–282 ms, 10 averages). The solid line indicates the fit to the signal envelope.

Finally, the fixed echo experiment was performed using a ten-phase cycle, selecting this time the $(-1,3)$ echo. The evolution delay was varied between 0.032 and 16.352 ms in 256 equidistant steps. The preparation delay was kept three times larger than the evolution time, ensuring the fixed echo location condition discussed above. The time-integral of the FIDs (estimated after discarding the first ten points) are shown versus the preparation time, for the small and large agar samples, together with their best fit (solid lines), in Fig. 9 (lower and upper part, respectively). By inspecting the formula Eq. (131), together with the imposed restriction $\tau 1 = 3\tau 2$, the fit function is obtained as

$$f(t) = a u_{31}^{1}(3\tau_2) u_{31}^{3}(\tau_2) = a\left(\exp\left\{-\frac{3\tau_2}{T_S}\right\} - \exp\left\{-\frac{3\tau_2}{T_F}\right\}\right)\exp\left\{-\frac{\tau_2}{T_S}\right\}.$$

5. Discussion

The use of the Liouville representation is well known in a broad area of physical applications. Since its first applications in pressure broadening phenomena, the formalism has been viewed as a convenient tool for deriving in a compact form the fundamental equations describing relaxation processes. Because NMR applications involve systems with few degrees of freedom, the Liouville representation could be used effectively in this context to obtain compact results. In this work, this approach is demonstrated for the relaxation of 3/2 spin systems in the presence of quadrupolar fluctuations. The first quantity of interest, the free propagator was constructed in a purely algebraic formulation as the exponential of the Liouvillian.

The main advantage of the superspace formalism in the context of spin 3/2 systems is that it yields the expression for the NMR signal as a sum over coherence pathways where all calculations are reduced to simple matrix multiplications (88). From this algebraic representation, the signal formula can be easily factored out as the product of four different components accounting for the effects of, RF amplitudes, RF phases, and B_0 and B_1 inhomogeneities. One important implication of this factorization is that the problem of determining accurate relaxation rates could be easily analyzed and, in particular, potential pitfalls and useful strategies could be derived.

The experimental results clearly demonstrated that the ubiquituous one-pulse experiments could produce reliable parameters only when carefully controlled experimental settings are considered and that, furthermore, for samples of irregular shape the effects of the spatial averaging for the B_0 and B_1 variations across its volume could lead to significant biases. These findings have strong implications for in vivo applications since for in vivo experiments the sample preparation is often outside of the experimenter's control. The two-pulse experiments, although more robust in nature, were also found to suffer from the effects of non-perfect spatial distributions in the B_0 and B_1 fields.

The three-pulse experiment was found to be the better choice for designing a non-biased experiment. Using a maximally filtered experiment, the amplitude of the signal is factored into a product of three terms, depending on B_1, B_0 and the relaxation properties, respectively. This observation was used to construct two classes of experiments, named here as variable and, fixed echo time experiments, respectively. These experimental designs were found to yield similar results and, in particular, the fixed echo experiments were found to have a signal to noise ratio advantage because the analysis of the data involves the

integral of the FID (in the variable echo experiments only the amplitude of the echo is measured). This advantage, however, could be compromised when in the presence of large B_0 inhomogeneities since under such conditions the FID decays rapidly as the measurement time gets further away from the echo position.

6. Conclusions

In this work, the usefulness of Liouville space representation in the study of relaxation has been demonstrated. This representation has been shown to be attractive not only because of its compact and elegant presentation of the theory, but also because it is an effective approach for the derivation of computationally efficient results. Results derived using this formalism were used to illustrate the potential biases in measured relaxation rates that could develop when measurements are performed in the presence of large B_0 inhomogeneities.

Appendix A

A.1. Superspace and spherical irreducible tensors

The simplest basis in superspace is given by the set of direct products of pure states, $|jm\rangle\langle jn|$, denoted using a convenient notation introduced in [22], $|mn^{\dagger}\rangle\rangle$. The decomposition of the identity in H provides the representation of any operator in terms of its matrix elements

$$\begin{aligned} O &= \sum_{m=-j}^{j}\sum_{n=-j}^{j}|jm\rangle\langle jm|O|jn\rangle\langle jn| \\ &= \sum_{m=-j}^{j}\sum_{n=-j}^{j}\langle jm|O|jn\rangle(|jm\rangle\langle jn|), \end{aligned} \tag{A.1}$$

which is rewritten in superspace language, as the decomposition of the associated supervector

$$|O\rangle\rangle = \sum_{m,n=-j}^{j}\langle jm|O|jn\rangle|mn^{\dagger}\rangle\rangle. \tag{A.2}$$

By convention, the hermitic conjugate of an operator

$$O^{\dagger} = \sum_{m=-j}^{j}\sum_{n=-j}^{j}(\langle jm|O|jn\rangle)^{*}(|jm\rangle\langle jn|)^{\dagger}, \tag{A.3}$$

corresponds to the "bra" in superspace,

$$\langle\langle O| \equiv \sum_{m,n=-j}^{j}\langle\langle mn^{\dagger}|(\langle jm|O|jn\rangle)^{*}. \tag{A.4}$$

This formula reaffirm the fact that the "bra" is the Liouville space hermitic conjugate of the corresponding "ket." The natural inner product is consistent with the "bra"–"ket" convention

$$\begin{aligned} \langle\langle mn^{\dagger}|O\rangle\rangle &= \langle jn|O|jm\rangle \quad \text{and} \quad \langle\langle O|mn^{\dagger}\rangle\rangle \\ &= (\langle jm|O|jn\rangle)^{*}. \end{aligned} \tag{A.5}$$

Using the $3j$ Wigner coefficients $\begin{pmatrix} j & k & l \\ m & n & p \end{pmatrix}$, the SITs can be written explicitly in terms of the direct product of basis for H (23)

$$\begin{aligned} |kq\rangle\rangle = &\sum_{|m|<j,|m+q|<j}(-1)^{j-(m+q)}\sqrt{2k+1} \\ &\times\begin{pmatrix} k & j & j \\ q & m & -(m+q) \end{pmatrix}|j,m+q\rangle\langle jm|. \end{aligned} \tag{A.6}$$

For the SIT operators, their associated superoperators are then given by the sum

$$\begin{aligned} \mathbf{T}_{lm} = &\sum_{k=1}^{3}\sum_{q=-k}^{k}\sum_{k'=|m+q|}^{3}(-)^{2j-m-q}\Delta(l,k,k') \\ &\times\begin{pmatrix} l & k & k' \\ m & q & -m-q \end{pmatrix}|k',m+q\rangle\rangle\langle\langle kq|, \end{aligned} \tag{A.7}$$

where the modified $9j$ Wigner symbol has been introduced for the sake of simplicity

$$\begin{aligned} \Delta(l,k,k') = &[(-)^{l+k+k'}-1]\sqrt{(2l+1)(2k+1)(2k'+1)} \\ &\times\begin{Bmatrix} l & k & k' \\ j & j & j \end{Bmatrix}. \end{aligned} \tag{A.8}$$

From the Jacobi identity

$$[A,[B,C]]+[B,[C,A]]+[C,[A,B]]=0, \tag{A.9}$$

the fact that the associated superoperator of a commutator is the commutator of the corresponding superoperators is obtained

$$[\mathbf{A},\mathbf{B}]|C\rangle\rangle = [A,[B,C]]-[B,[A,C]] = [[A,B],C]. \tag{A.10}$$

As a consequence, the SIT *superoperators* satisfy with the angular momentum superoperators, the same commutation relations as their operator counterparts

$$\begin{aligned} &[\mathbf{J}_Z,\mathbf{T}_{lm}] = m\mathbf{T}_{l,k}, \\ &[\mathbf{J}^{\pm},\mathbf{T}_{lm}] = \sqrt{l(l+1)-m(m\pm1)}\mathbf{T}_{l,m\pm1}. \end{aligned} \tag{A.11}$$

The structure constants are directly related with the superoperator matrix elements

$$[T_{lm},T_{\lambda\mu}] = \mathbf{T}_{lm}|\lambda\mu\rangle\rangle = \sum T_{k,m+\mu}\langle\langle k,m+\mu|\mathbf{T}_{lm}|\lambda\mu\rangle\rangle \tag{A.12}$$

and they are shared with their superoperators counterparts

$$[\mathbf{T}_{lm},\mathbf{T}_{\lambda\mu}] = \sum\mathbf{T}_{k,m+\mu}\langle\langle k,m+\mu|\mathbf{T}_{lm}|\lambda\mu\rangle\rangle. \tag{A.13}$$

The most important property of the associated superoperator **A** of a "standard" operator A in NMR applications is obtained as a direct consequence of the Baker–Hausdorff–Campbell formula

$$\exp(A)B\exp(-A)=\sum_{k=0}^{\infty}\frac{1}{k!}[A,[\ldots[A,B]]]. \tag{A.14}$$

Recognizing in the RHS the exponential series for the superoperator $\mathbf{A}$ we have

$$\exp(\mathbf{A})|B\rangle\rangle=|\exp(A)B\exp(-A)\rangle\rangle. \tag{A.15}$$

A.2. Appendix propagator matrix elements

Using the short form introduced in (16), the auxiliary projectors are given by

$$\mathbf{P}_{01}=\frac{1}{5}\begin{pmatrix}1&0&2\\0&0&0\\2&0&4\end{pmatrix}\mathbf{e}_0,\quad \mathbf{P}_{02}=\frac{1}{5}\begin{pmatrix}4&0&-2\\0&0&0\\-2&0&1\end{pmatrix}\mathbf{e}_0,$$
$$\mathbf{P}_{03}=\begin{pmatrix}0&0&0\\0&1&0\\0&0&0\end{pmatrix}\mathbf{e}_0, \tag{A.16}$$

$$\mathbf{P}_{04}=(\mathbf{e}_1+\mathbf{e}_{-1})\frac{1}{5}\begin{pmatrix}2&0&-\sqrt{6}\\0&0&0\\-\sqrt{6}&0&3\end{pmatrix}+(\mathbf{e}_3+\mathbf{e}_{-3}), \tag{A.17}$$

$$\mathbf{K}_{11}=(\mathbf{e}_{-2}-\mathbf{e}_2)\frac{1}{2}\begin{pmatrix}0&1\\1&0\end{pmatrix},$$
$$\mathbf{K}_{12}=(\mathbf{e}_{-2}-\mathbf{e}_2)\frac{1}{2}\begin{pmatrix}0&-\mathrm{i}\\\mathrm{i}&0\end{pmatrix}, \tag{A.18}$$
$$\mathbf{K}_{13}=(\mathbf{e}_2+\mathbf{e}_{-2})\frac{1}{2}\begin{pmatrix}1&0\\0&-1\end{pmatrix},$$

$$\mathbf{K}_{21}=\frac{\sqrt{5}}{10}\begin{pmatrix}0&\sqrt{3}&0\\\sqrt{3}&0&\sqrt{2}\\0&\sqrt{2}&0\end{pmatrix}(\mathbf{e}_{-1}-\mathbf{e}_1),$$
$$\mathbf{K}_{22}=\frac{\mathrm{i}\sqrt{5}}{10}\begin{pmatrix}0&\sqrt{3}&0\\-\sqrt{3}&0&-\sqrt{2}\\0&\sqrt{2}&0\end{pmatrix}(\mathbf{e}_1-\mathbf{e}_{-1}), \tag{A.19}$$

$$\mathbf{K}_{23}=\frac{-1}{10}\begin{pmatrix}3&0&\sqrt{6}\\0&-5&0\\\sqrt{6}&0&2\end{pmatrix}(\mathbf{e}_1+\mathbf{e}_{-1}). \tag{A.20}$$

With the notations

$$\begin{cases}C_\alpha=\mathrm{e}^{-j_\alpha t}\cosh(t\Delta_\alpha)\\ S_\alpha=\mathrm{e}^{-j_\alpha t}\frac{\sinh(t\Delta_\alpha)}{\Delta_\alpha}\end{cases},\quad \Delta_\alpha=\sqrt{j_\alpha^2-\omega_Q^2}, s(t)=\mathrm{e}^{-2j_2t},\quad f(t)=\mathrm{e}^{-(j_0+j_2)t}, \tag{A.21}$$

the matrix elements of the free propagator are displayed here, together with their values in the limit case $j_1\to j_2$ and $\omega_Q\to 0$

$$\begin{aligned}
u_{11}^0&=\tfrac{1}{5}\mathrm{e}^{-2j_1t}+\tfrac{4}{5}\mathrm{e}^{-2j_2t}\to s(t) & u_{22}^2&=\mathrm{e}^{-(j_0+j_2)t}(C_1-j_1S_1)\to f(t)s(t)\\
u_{22}^0&=\mathrm{e}^{-2(j_1+j_2)t}\to s^2(t) & u_{32}^2&=-\mathrm{i}\omega_Q\mathrm{e}^{-(j_0+j_2)t}S_1\to 0\\
u_{33}^0&=\tfrac{4}{5}\mathrm{e}^{-2j_1t}+\tfrac{1}{5}\mathrm{e}^{-2j_2t}\to s(t) & u_{33}^2&=\mathrm{e}^{-(j_0+j_2)t}(C_1+j_1S_1)\to f(t)\\
u_{31}^0&=\tfrac{2}{5}(\mathrm{e}^{-2j_1t}-\mathrm{e}^{-2j_2t})\to 0 & u_{33}^3&=\mathrm{e}^{-(j_1+j_2)t}\to s(t)
\end{aligned} \tag{A.22}$$

$$\begin{aligned}
u_{11}^1&=\frac{2}{5}\mathrm{e}^{-(j_1+j_2)t}+\frac{3}{5}\mathrm{e}^{-(j_0+j_1)t}(C_2+j_2S_2)\to\frac{2}{5}s(t)+\frac{3}{5}f(t)\\
u_{21}^1&=-\mathrm{i}\sqrt{\frac{3}{5}}\mathrm{e}^{-(j_0+j_1)t}\omega_QS_2\to 0\\
u_{31}^1&=-\frac{\sqrt{6}}{5}\mathrm{e}^{-(j_1+j_2)t}+\frac{\sqrt{6}}{5}\mathrm{e}^{-(j_0+j_1)t}(C_2+j_2S_2)\to\frac{\sqrt{6}}{5}(f(t)-s(t))\\
u_{22}^1&=\mathrm{e}^{-(j_0+j_1)t}(C_2-j_2S_2)\to f(t)s(t)\\
u_{32}^1&=-\mathrm{i}\sqrt{\frac{2}{5}}\mathrm{e}^{-(j_0+j_1)t}\omega_QS_2\to 0\\
u_{33}^1&=\frac{3}{5}\mathrm{e}^{-(j_1+j_2)t}+\frac{2}{5}\mathrm{e}^{-(j_0+j_1)t}(C_2+j_2S_2)\to\frac{3}{5}s(t)+\frac{2}{5}f(t)
\end{aligned} \tag{A.23}$$

References

[1] G. Navon, Complete elimination of the extracellular Na NMR signal in triple quantum filtered spectra of rat hearts in the presence of shift reagents, Magn. Reson. Med. 30 (4) (1993) 503–506.

[2] I. Hancu et al., In vivo single and triple quantum filtered ^{23}Na MRI of brain neoplasms, in: 8-th Sci Meeting ISMRM, Denver, 2000.

[3] S. Hilal et al., Sodium imaging in magnetic resonance imaging, in: D. Stark, W. Bradley (Eds.), Mosby, St. Louis, 1992, 1091–1110.

[4] F.E. Boada et al., Fast three dimensional sodium imaging, Magn. Reson. Med. 37 (5) (1997) 706–715.

[5] I. Hancu, F.E. Boada, G.X. Shen, Three-dimensional triple-quantum-filtered Na imaging of in vivo human brain, Magn. Reson. Med. 42 (6) (1999) 1146–1154.

[6] A. Borthakur et al., In vivo triple quantum filtered twisted projection sodium mri of human articular cartilage, J. Magn. Reson. 141 (2) (1999) 286–290.

[7] A.G. Redfield, On the theory of relaxation processes, IBM J. Res. Dev. 1 (1957) 19–31.

[8] U. Fano, Description of states in quantum mechanics by density matrix and operator techniques, Rev. Mod. Phys. 29 (1) (1957) 74–93.

[9] v.H. Primas, Eine verllagemeinerte Storrungstheorie fur quanten-mechanische Mehrteilchenprobleme, Helv. Phys. Acta 34 (1960) 330–351.

[10] H. Gabriel, Theory of the influence of environment on the angular distribution of nuclear radiation, Phys. Rev. 181 (2) (1969) 506–521.

[11] A. Ben-Reuven, Symmetry considerations in pressure-broadening theory, Phys. Rev. 141 (1) (1966) 34–40.

[12] I. Hancu, J.v.d. Maarel, F. Boada, A model for the dynamics if spins 3/2 in biological media: signal loss during radio-frequency excitation in triple-quantum-filtered sodium MRI, J. Magn. Res. 147 (2000) 179–191.

[13] C.P. Slichter, Principles of magnetic resonance, third ed., Springer Series in Solid State Sciences, Springer, 1996, 655.

[14] W.E. Palke, J.T. Gerig, Relaxation in presence of an RF field, Concepts Magn. Reson. 9 (5) (1997) 347–353.

[15] G.J. Bowden, W.D. Hutchinson, J. Khachan, Tensor operator formalism for multiple-quantum NMR. Spins 3/2, 2 and 5/2 and general I, J. Magn. Res. 67 (1986) 415–437.

[16] P.S. Hubbard, Quantum-Mechanical and Semiclassical Forms of the Density Operator Theory of Relaxation, Rev. Mod. Phys. 33 (2) (1961) 249–264.
[17] A. Abragam, Principles of nuclear magnetism, in: W. Marshall, D. Wilkinson (Eds.), International Series of Monographs on Physics, Oxford University Press, New York, 1978, p. 599.
[18] G. Bodenhausen, H. Kogler, R.R. Ernst, Selection of coherence-transfer pathways in NMR pulse experiments, J. Magn. Reson. 58 (3) (1984) 370–388.
[19] M. Kim, S. Lee, Spin echoes after arbitrary N pulses, J. Magn. Reson. 125 (1) (1997) 114–119.
[20] P.A. Keifer, 90 Pulse width calibrations: how to read a pulse width array, Concepts Magn. Reson. 11 (3) (1999) 165–180.
[21] S.P. Brown, S. Wimperis, NMR measurement of spin-3/2 transverse relaxation in an inhomogeneous B1 field, Chem. Phys. Lett. 224 (5-6) (1994) 508–516.
[22] M. Baranger, Simplified quantum-mechanical theory of pressure broadening, Phys. Rev. 111 (2) (1958) 481–493.